Sensor design for the CMS Silicon Strip Tracker

L. Borrello, E. Focardi, A. Macchiolo, A. Messineo

October 5, 2002

1 Introduction

The Silicon Strip Tracker (SST) constitutes, in conjunction with the Pixel Tracker, the inner tracking of the Compact Muon Solenoid (CMS) experiment. The SST is composed of about 19000 500 μm and 6000 320 μm thick, large area single sided silicon strip "p-on-n" sensors. The cristal lattice orientation will be of <100> type.
This note is aimed to describe the design of the silicon sensors, for the different detector topologies foreseen by the SST.

2 General design features

Both the 500 μm thick ("thick") silicon sensors and the 320 μm thick ("thin") sensors will be manufactured using 6" technology, with the standard planar process usually employed in the IC industry. One single detector is produced from each wafer and it is requested to lie inside a fiducial circle of about 13.9 cm diameter.
The wafer thickness must be within 20 μm of the specification, the flatness such that the wafer warp is less than 100 μm, the dicing accuracy at the level of 20 μm. The mask alignment tolerance is 1 μm, as the requested precision of the implants dimensions.

An uniform, metallized, n^+ layer is present on the sensor backside providing an ohmic contact between the bulk and the metal contact. Moreover, the presence of this highly doped n^+ layer acts as a barrier for minority carriers

coming from the depleted bulk and for majority carriers injected from the metal contacts, keeping the overall leakage current very low. In addition, on the junction side, an n^+ implant is required along the edges of the device, in order to prevent the space charge region from reaching the cutting edge, thus protecting the active area from injection of charges originating in this heavily damaged region.
The distance of the implanted region from the cutting edge, d $\approx 2\times$ thickness $+ 110$ μm, minimizes the occurence of breakdown phenomena.

The active region is surrounded by two p^+ rings. The external one prevents the flowing of leakage current from the sensor edges to the internal ring, used to bias the strips. The metal field plates extend beyond the implantation, to avoid high fields at its edge. The very large metal over-hang on the guard ring external side acts actually as a multi-guard structure, allowing electric field smoothing. Also the ring geometry, with rounded corners, helps to avoid discharges while operating the device at high voltage.
In order to simplify testing and biasing procedures the bias and guard ring dimensions perpendicular to the strip direction are wider than the hortogonal ones.

The passivation of the front side improves the detector stability and reduces the handling fragility.
The producers are requested to supply sensors polished in the front and acid etched in the back side.

A p^+ implantation is performed on the front side in order to define the strip-shaped diode. The width of the implant strips depends on the strip pitch; a constant width/pitch of 0.25 is used. This value is a compromise between an high width/pitch ratio that reduces the field peak located at the p^+ edge and a low value of the ratio that enhances the resolution and keeps the total strip capacitance low. Aluminum read-out strips, capacitatevely coupled over the p^+-implants, will be 15 % wider than the width of the implant underneath. The overhang ranges from 4 to 8 μm, depending on the strip pitch. As in the case of the bias and guard rings, this design choice will move the high edge electric field from the silicon into the much more resistant oxide layer, reducing the risk of electrical breakdown. The thickness of the metal layer is required to be greater than 1.2 μm to limit the noise contribution due to the resistance of the electrode.
An array of polysilicon resistors is used to bias the implant strips; these resistors are aligned and connected to each strips from the bias ring, on the same side of the sensor, where a metallised probe pad (DC pad), contacting the implant, is foreseen. The choice of poly-silicon as biasing technique is mainly

due to its established radiation resistance, and it relies on the capability of producers in defining the resistance value by means of controlled doping by implantation or diffusion. The resistor value is requested to be 1.5 $\pm$ 0.5 MΩ.
The producers are left free to choose the appropriate technology for the integrated coupling capacitors provided that they are able to satisfy the requirements on the number of defective strips. Both manufacturers have implemented multiple thin layers of SiO_2 and Si_3N_4. A thicker oxide fills the interstrip gap.
Two rows of AC pads are used at the edges of the strips on each side of the detector to allow for bonding and testing. In the rectangular sensors and in most of the wedge-shaped ones the pad step has been kept constant. An examples of how the different structures are arranged in the active region is shown in Fig. 1.

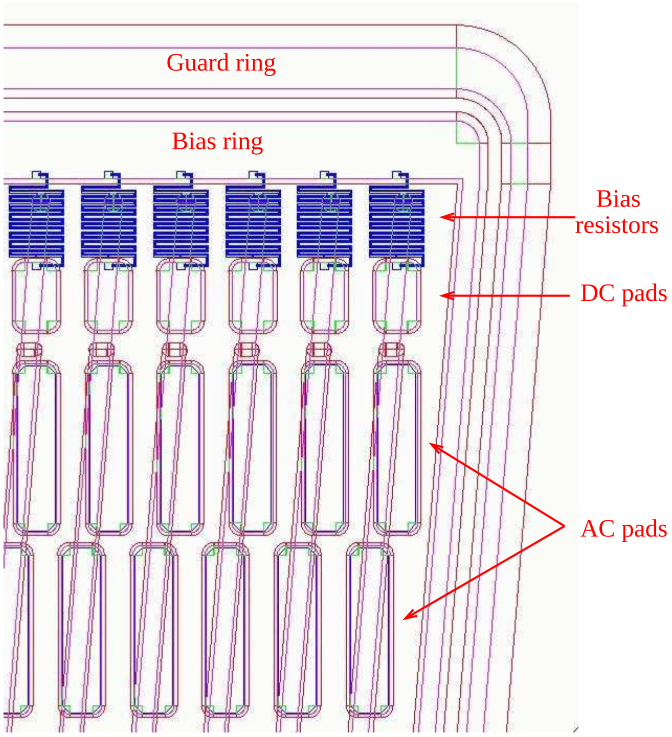

Figure 1: View of one edge of the active region in the W3 detector.

A series of reference marks is drawn in the n^+ implanted region, for assembling and mechanical survey purposes. Every sensor is identified by a binary code created by scratching dedicated pads in the non-active region. A similar identification scheme is requested in the test-structures area.

3 Sensor geometries

The CMS tracker sensors are foreseen in 15 different geometries: two rectangular detectors for the TIB (see dimensions in Tab.1), two for the TOB (Tab.2), eleven wedge-shaped detectors for the TID and the TEC (Tab.3). Each detection unit in the inner region (TIB, TID and the first four ring of TEC) is composed by a single micro-strip sensor, and by two daisy-chained sensors in the outer region (TOB and the last three rings of TEC). The first two layers in TIB and TOB, the first two rings in TID and TEC and rings 1,2, 5 in TEC are instrumented with double-sided modules. These are made with two independent single-sided detection units, mounted back to back, with the second one being rotated of 100 mrad with respect to the first.
All over the Tracker the strip pitch varies from the inner to the outer layers. The pitch is tuned in order to match the electronic modularity of 256 channels. Moreover the range of the chosen strip pitch is also driven by two particle separation and the achievable two-hit resolution, whereas the range of strip lenghts is driven by minimum bias occupancy and noise levels.
The wedge detectors measuring the ϕ-coordinate are designed, ring by ring, with the strips pointing to the interaction point. This results in a constant angular pitch in each ring and in a slightly varying linear pitch along the two basis.

Type	L1 active/phys.	L2 active/phys.	H	Pitch	strips	multipl.
IB1	61.5 /63.3	61.5 /63.3	116.9 /119.0	80	768	1536
IB2	61.5 /63.3	61.5 /63.3	116.9 /119.0	120	512	1188

Table 1: Inner Barrel thin sensors (320 $\pm$ 20 μm): IB1 will be mounted on 768 double-sided modules in the two inner layers of the TIB, IB2 in 1188 single modules in the two outer layers. Multiplicities do not take into account the spare sensors.

Type	L1 active/phys.	L2 active/phys.	H	Pitch	strips	multipl.
OB1	93.9 /96.4	93.9/96.4	91.6/94.4	122	768	3360
OB2	93.9 /96.4	93.9/96.4	91.6/94.4	183	512	7056

Table 2: Outer Barrel thick sensors (500 $\pm$ 20 μm): OB1 will be mounted on 1680 single-sided modules in the layers 5 and 6 of the TOB, OB2 in the inner TOB layers (1-4) in single and double modules. All the TOB detectors are composed by two daisy-chained sensors.

Thick sensors will be supplied to the Tracker Collaboration by STM and thin sensors by HPK. They differ for the distance from the active region to

Type	L1 active/phys.	L2 active/phys.	H	Pitch	strips	multipl.
W1 TEC	63.1 /64.6	85.8/87.9	85.2/87.2	81/112	768	288
W1 TID	62.1 /63.6	91.7/93.8	110.9/112.9	80.5/119	768	288
W2	86.6 /112.2	110.1/112.2	88.2/90.2	113/143	768	864
W3	63.3 /64.9	81.1/83.0	110.7/112.7	123/158	512	880
W4	58.1/59.7	71.3/73.2	115.2/117.2	113/139	512	1008
W5a	96.5/98.9	109.5 /112.3	81.2/84.0	126/142	768	1440
W5b	110.0/112.5	120.1/122.8	63.2/66.0	143/156	768	1440
W6a	83.6/86.1	94.6/97.4	96.1/99.0	163/185	512	1008
W6b	94.5/97.5	104.7/107.5	84.9/87.8	185/205	512	1008
W7a	71.5/74.0	80.1/82.9	106.9/109.8	140/156	512	1440
W7b	80.4/82.9	88.0/90.8	94.9/90.8	156/172	512	1440

Table 3: Thin (W1-W4) and thick (W5a-W7b) wedge sensors for TID and TEC: W1 has two different versions for TID and TEC, whereas the TID shares identical W2 and W3 sensors with the TEC. W1, W2 and W5 will be assembled in double sided modules, the other geometries in single-sided modules.

the sensor edge, calculated on the basis of the wafer thickness, and for slight variations in the dimensions of the bias and guard ring, of the DC and AC pads, of the bias resistors, in the shape of the reference marks and of the openings in the passivation layer.
Details of the process are under the provider responsability and hence can vary for thin and thick sensors, as far as the fabrication process is kept constant for all the production.

4 Test structures

The wafer hosts additional devices beyond the main detector, designed to monitor the stability of the technology. A standard set of nine structures, requested by the Tracker Collaboration, is placed inside the fiducial region (standard half-moon) and it is shown in Fig.2. The design is identical for the two supplier. From left to right it is composed by:

- Ts-Cap, an array of 26 AC coupled strips, with a pitch of 122 μm, characterised by the same dielectric composition of the main sensor but with a direct connection to the bias ring, without polysilicon resistors. Each strip, 30 μm large and 4413 μm long, can be read from an AC pad that is placed alternatively on the two opposite bases. This device is used to analyse the quality of the dielectric, with the measurement of its breakdown voltage and of the decoupling capacitance value.

- Sheet, composed by 9 superficial structures, to measure sheet resistance: 3 implant strips, 3 aluminum strips, 3 poly-silicon resistors, all

lying directly on the n-doped bulk. All the 9 structures have a separate contact on one side of the device, whereas on the opposite end they are connected to the bias ring.
The three poly-silicon resistors are exactly equal to the ones that we find on the real sensors. The resistivity of the aluminum and of the p^+ implant is estimated with two sets of strips, each containing 3 strips, 50, 20 and 10 μm large and approximately of the same length. The mask design has exactly the same number of squares for the 3 aluminum and the 3 p^+ strips of the same width. For STM test-structures this equality has been maintained, whereas for HPK the number of squares varies slightly between aluminum and p^+ because the production process results in a reduction of 1 μm in the width of metal layer and in an increase of 1 μm in the width of the p^+ implant with respect to the mask dimensions.
In the case of the Al resistivity, also the contribution of the bias ring length comprised between the strip end and the probe contact to the total number of squares must be considered (see Tab.4).

	HPK	STM
width p^+ strip N.1	12	10
numb. of square p^+ strip N.1	727	872
width p^+ strip N.2	22	20
numb. of square p^+ strip N.2	399	438
width p^+ strip N.3	52	50
numb. of square p^+ strip N.3	172	179
width Al strip N.1	8	10
numb. of square Al strip N.1	1087	872
width Al strip N.2	18	20
numb. of square Al strip N.2	486	438
width Al strip N.3	48	50
numb. of square Al strip N.3	185	179
numb. of Al squares added by the BR	31	25

Table 4: Dimensions of some of the Sheet structures. In case of the Al resistivity measurement the contribution of the bias ring has to be added.

- Gate Controlled Diodes: this structure hosts 4 GCDs, two circular ones on the upper side and two square ones in the bottom side. In the square geometry, one of the GCDs is composed by a comb shaped MOS intertwined with a comb made of poly-silicon strips. In the second one the poly-silicon strips are replaced by p^+ implanted strips.

- Cap-Ts-Ac, a device built of two sets of 9 strips with the same structure of the main sensor. In one of them, the poly-silicon resistors are

aligned on the same side, on the second one they are alternatively on the two sides of the device.
This structure is aimed to measure the interstrip capacitance between the central strip in each group of nine, and the two neighbouring ones. The three external strips on each side are connected through their metallization, to facilitate their grounding.
The strip width is 30 μ, the lenght 10170 μm and the pitch 122 μm.

- Standard mini-sensor: a small-size replica of the main sensor. It is a rectangular detector, with an active area of 2.3×1.6 cm^2, composed by 192 strips, at a pitch of 120 μm, that is an average value among the pitches of the different sensor geometries characterizing the CMS Tracker sensors. The dimensions of the bias and of the guard rings, and the apertures in the passivation layers over them, vary slightly between thin and thick wafers, reflecting the geometries adopted for these structures in STM and HPK sensors. The second rows of AC pads is displaced by 2 mm with respect to bias-ring, in order to perform bonding tests.

- Cap-Ts-Dc has been designed to measure interstrip resistance. Its structure is similar to Cap-Ts-Ac, except for the fact that the strips are not connected to the bias ring, either directly or through a bias resistor. In addition the dielectric layer is missing in the strips and the p^+ implant can be contacted all over their lenght.

- A simple square diode, of area 0.24 cm^2, surrounded by a guard ring.

- Two Mos devices with a gate area of 0.24 cm^2. For both the Mos devices included in the HPK structures and for the first MOS in STM wafers, the dielectric composition corresponds to the thick oxide layer that is present in the interstrip region in the main detector. In the second STM Mos the dielectric layer follows the structure of the decoupling capacitance in the detector strips. It is hence made of thin layers of SiO_2 and Si_3N_4.

An additional mini-sensor is present in each wafer. It is designed with the same pitch and pad arrangment of the main detector on the read-out side, in such a way that it may be used for tests on bonding and on the read-out electronics. It is characterised by a reduced lenght and a smaller number of strips with respect to the main sensor, depending on the available space left on the wafer.

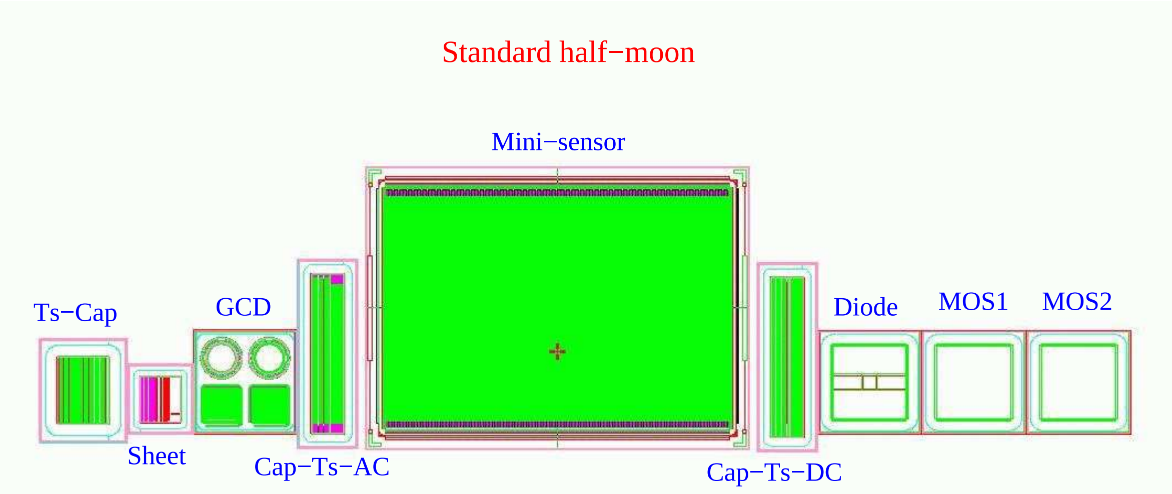

Figure 2: View of the set of 9 test structures called "standard half-moon"

5 HPK Silicon Sensors

- **Wafer layout:** HPK sensors are placed in the wafer inside a fiducial region, shaped as a circle of 139480 μm diameter (see Fig. 3 for example). Additional structures are present along the four sides of the main sensor: the standard half moon (described in Section 4), Mos devices and diodes to check for the quality of the substrate and of the oxide layer, the mini-sensor.

- **Strip structure:** The widths of the p$^+$ and metal layer of the strips in all the sensor types follow the rules described in Section 2. The metal over-hang is 6 μm in the DC pads and 5 μm in the AC pads. The openings in the passivation layer on the DC and AC pads are inside the region defined by the implant layer, as requested by the provider. These apertures define the available space for testing and bonding on the pads. The AC pads have an additional layer of poly-silicon, covering the not passivated region. The strips have rounded borders both in the implant and in the metal layer. The distance between the end of the strips and the bias ring, on the sides perpendicular to the strip direction, is 30 μm in the implant layer. The distance between the external strips and the bias ring on the side along the strip direction,

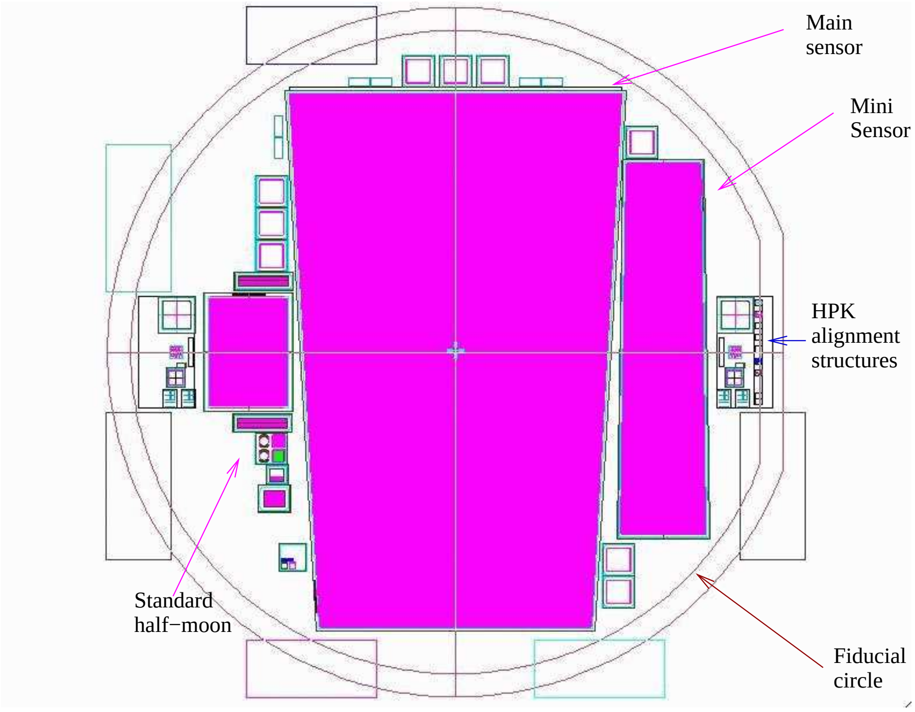

Figure 3: Lay-out of the HPK wafer for the W4 detector

depends on the sensor type. The strip implant runs also below the poly-silicon bias resistor. The bias resistors are always aligned on the same side. In the HPK sensors they follow two basic designs: R_1, implemented in the W3 sensor, and R_2, for all the other detectors. Resistor dimensions are listed in Table 5. In the mini-sensor included in the standard half-moon the bias resistor is of the R_2 type, since this is the most common design among the HPK detectors.

Resistor type	Lenght	Width	Number of squares
R_1	200	120	413
R_2	400	70	422

Table 5: Characteristics of the two bias resistor types present in the HPK sensors

- **Bias and Guard ring:** the structure and the width of the bias and guard ring are the same for all the sensors provided by HPK. Dimensions are summarized in Tab. 6. The openings in the passivation layer on the bias ring run for all the lenght of the sides perpendicular to the strip direction and they cover the lenght of the pads on the sides parallel to the strip direction. The guard ring has openings in the passivation layer only in the four corners of its structure (see Fig. 4). The bias and the guard rings have rounded corners except for the most internal implant and metal lines, defining the active region.

	Implant width	Metal over-hang on the internal side	Metal over-hang on the external side
Bias Ring (side perpendicular to the strip direction)	130	8	18
Bias Ring (side along the strip direction)	39	8	18
Guard Ring (side perpendicular to the strip direction)	92	18	48
Guard Ring (side along the strip direction)	39	18	48

Table 6: Dimensions of the Bias and Guard Rings in the HPK sensors

- **Structure of the detector non-sensitive region:** The distance between the external edge of the p^+ implant on the guard ring and the internal side of the n^+ zone is 300 μm on all the detector sides. The width of the n^+ region is 450 μm, with a metal over-hang in the internal edge of 50 μm and in-hang of 20 μm in the external edge. The passivation layer is opened along the cut region. The strip numbers and the reference figures for alignment are designed as apertures in the metal layer over the n^+ region. The reference figures are L-shaped with a side lenght of 800 μm for the rectangular sensors (IB1 and IB2) and of 600 μm for the wedge sensors (W1 to W4), as shown in Fig. 5. In the figure also the numbering scheme is visible with the numbers growing from left to right when the side with poly-silicon resistors is on the upper part of the sensor.

5.1 Review of the characteristics of HPK sensor type

The geometrical dimensions of all the sensor types are given in the schematics of the mask designs included in this note (Fig. 23-36). Only the peculiarities of each detector design are illustrated in the following.

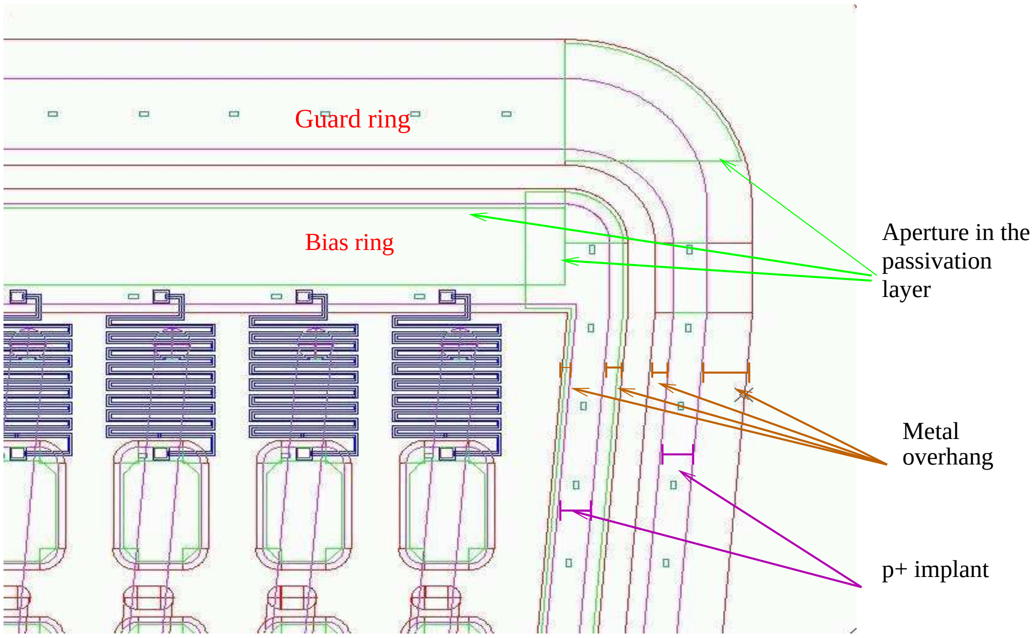

Figure 4: Structure of the bias and guard ring for the HPK sensors.

- **IB1:** IB1 is a rectangular detector designed with 768 strips at a pitch of 80 μm, the narrowest one among all the 14 different geometries of the CMS silicon sensors in the read-out side. It will be mounted on 768 double-sided modules in the two inner layers of the TIB.
  The width of the implant strip is 20 μm, and the width of the strip metallization 28 μm. The choice to align all the bias resistors on the same side has led to the need of decreasing the width of the DC pads with respect to the other sensor types (the opening in the passivation layer is 62 μm large). The AC pads are staggered in two different rows for adiacent strips, allowing to keep the pads large enough for bonding purposes. In this way the total number of AC pad rows on either side of this sensor sums to 4. The arrangment of the pads on the strips is shown in Fig. 6.

  The IB1 mini-sensor is designed with the active region 80000 μm long and 128 strips.

- **IB2:** IB2 has identical external dimensions with respect to IB1 but only 512 strips, resulting in a pitch of 120 μm. This detector will be mounted on 1188 single modules in the two outer layers of the TIB.
  The width of the implant strip is 30 μm, and the width of the strip

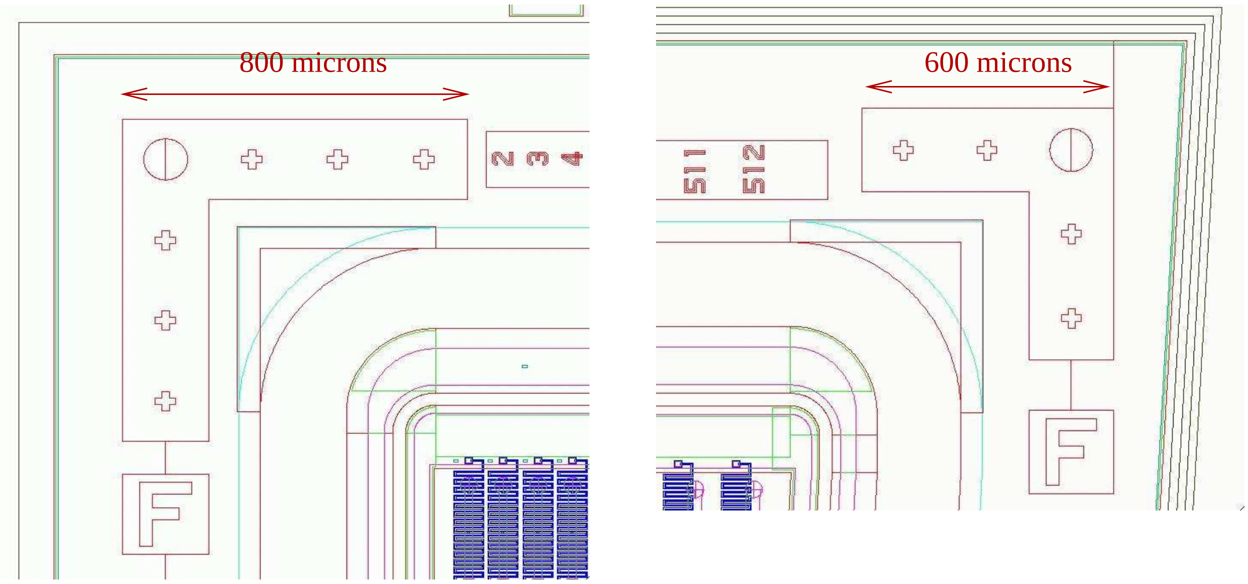

Figure 5: Reference figures, used for alignment: on the right in the case of the IB1 and IB2 detectors, on the left for the wedge sensors.

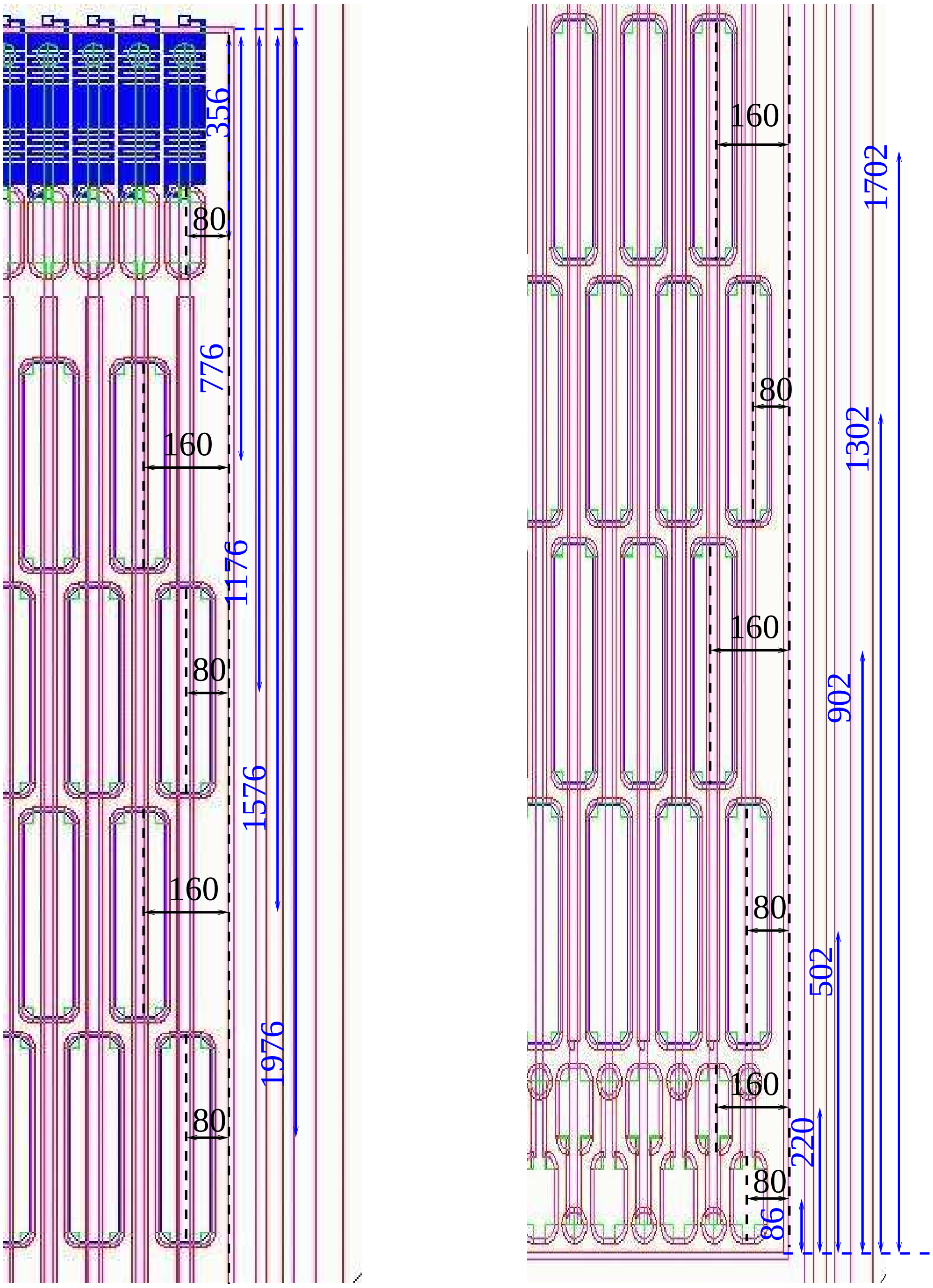

Figure 6: Views of the edges of the active region on the two opposite sides of the IB1 detector.

metallization 40 μm. The wider space available between strips has allowed to keep both DC and AC pads at the same level for adiacent strips, resulting in one DC pad row and two AC pad rows on either side of the detector (see Fig.7). In IB1 and IB2 all the strips are numbered. The IB2 mini-sensor has 64 strips and the active region is 50000 μm long.

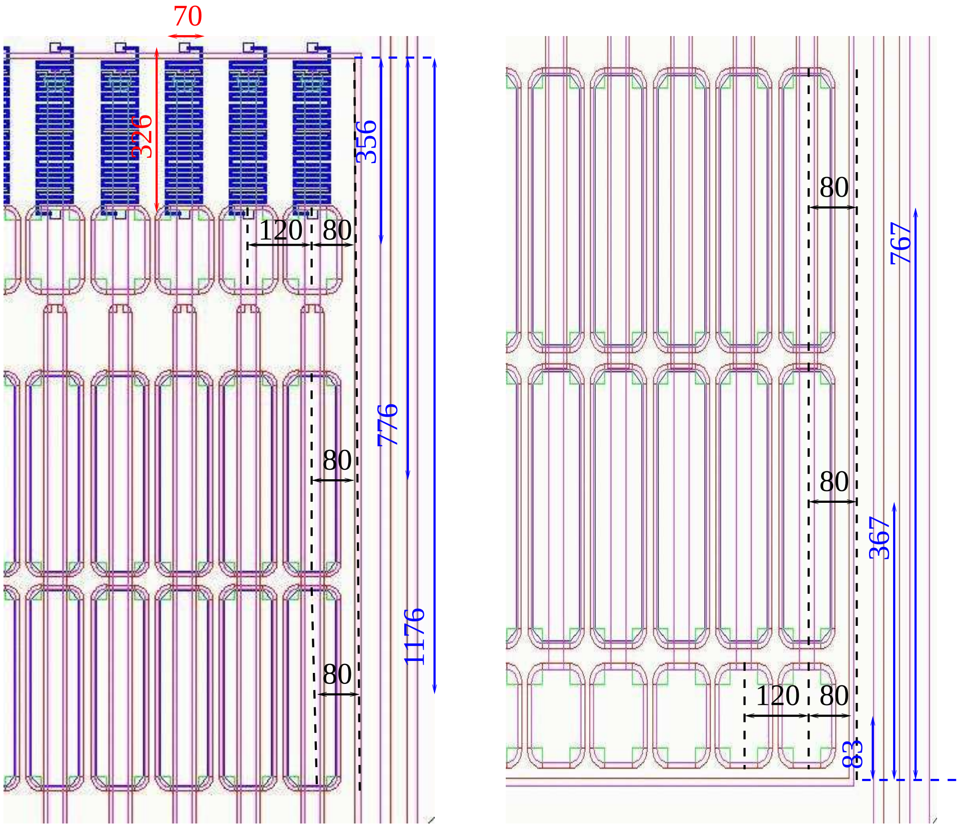

Figure 7: Views of the edges of the active region on the two opposite sides of the IB2 detector.

- **W1 TEC and W1 TID:** The first rings of the TEC and of the TID use detectors with the same angular pitch (0.019852°), but of different lenght. The TID sensor has been designed 25700 μm longer and at a lower inner radius (231300 μm instead of 235100 μm for W1 TEC) to fill regions where the SST would otherwise have no acceptance. The W1 detectors will be mounted on 144 double-sided modules, both in the TEC and in the TID, with 24 modules in ϕ in each of the 6 disks. In both the W1 detectors, it was not possible to arrange the DC and

AC pads at a constant step all along the detector width, since the linear pitch varies largely between the external and the internal strips. For example, in W1 TEC, the pitch between the most external strips is 112.8 μm, whereas between the two central strip is 111.0 μm. In order to keep the possibility of testing the sensor with a probe-card, we have chosen to build a group of pads, inside which the step is constant. This group is repeated all along the detector width, but the position of the first pad in the group is adjusted in such a way that all the pads contact the corresponding strips. So the pad step is constant everywhere except between the $(N \times i)$th and $(N \times i+1)$th pads, where N is the number of pads in the group and i is the group repetition index. In W1 TEC and W1 TID each group is made of 16 pads on the wedge wider base and 8 pads on the narrower one. Here the pad distance corresponds to twice the strip pitch, since the even and odd DC and AC pads are staggered in two different rows (Fig.8). The W1 TEC (TID) mini-sensor has 128 (64) strips and an active lenght of 80000 μm.

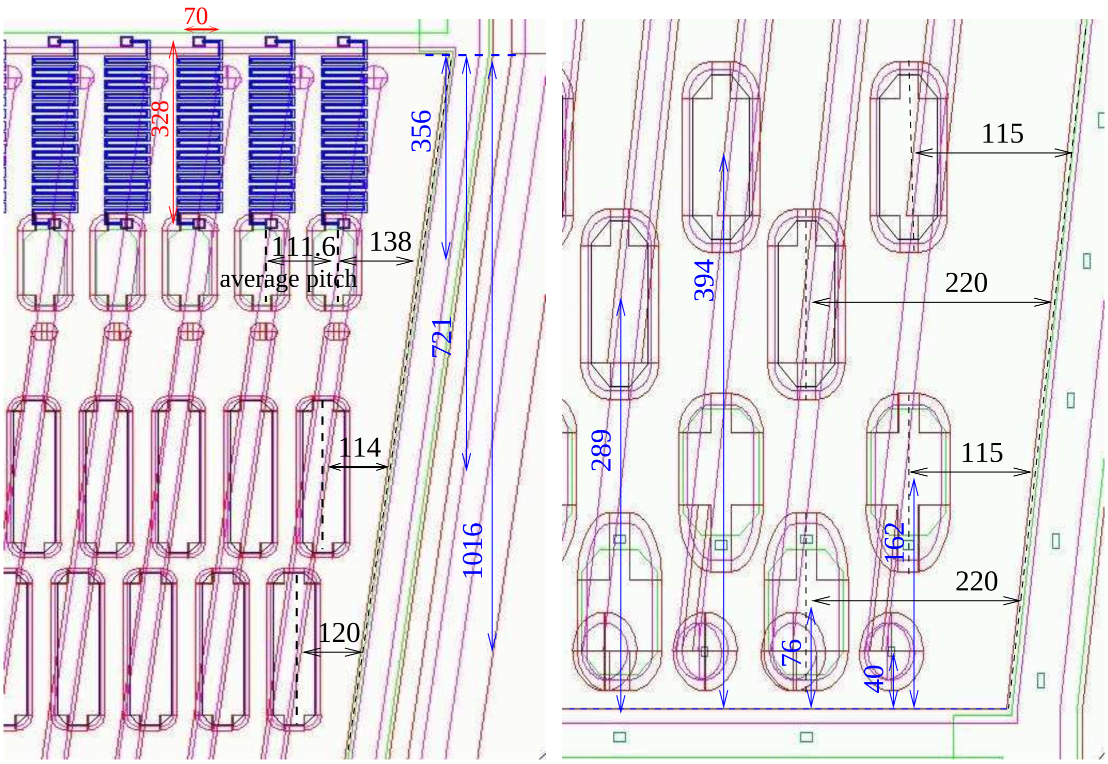

Figure 8: Views of the edges of the active region on the two opposite sides of the W1 TEC detector.

- **W2:** The W2 detector is the active element of the second ring in the TEC (288 double-sided modules) and of the TID (144 double-sided

modules, 24 modules in ϕ in each disk). The inner radius of the active region, measured at the internal edge of the bias ring, is 323000 μm, and the angular pitch 0.01985 °.
Also in this case it was not possible to keep a constant step among all the pads and a similar arrangement to the W1 one has been adopted. On both the sensors bases the pad groups are composed of 16 elements and the DC pads and the first row of AC pads are aligned along the vertical axis (Fig.9).
The W2 mini-sensor has 64 strips and an active lenght of 45000 μm.

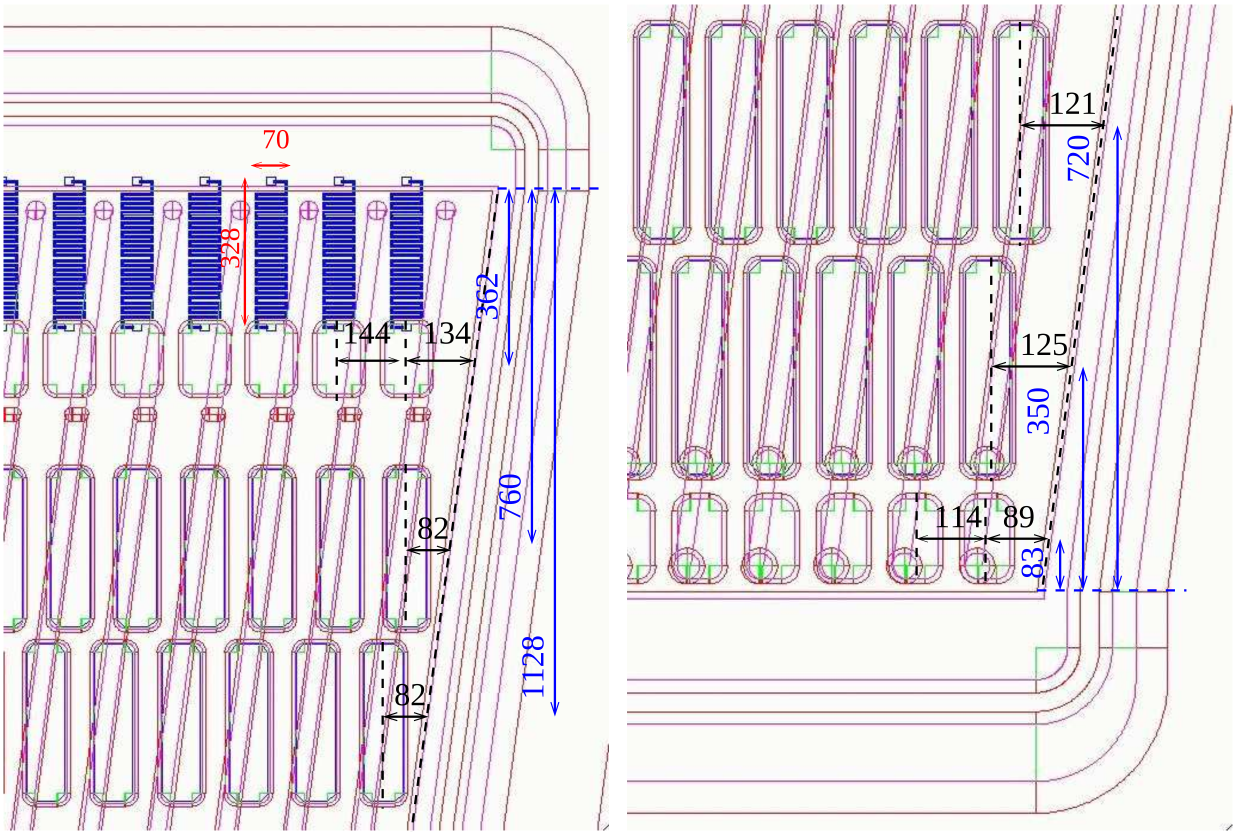

Figure 9: Views of the edges of the active region on the two opposite sides of the W2 detector.

- **W3:** This wedge detector, made of 512 strips, is the sensitive element of the third ring in the TEC (640 single modules, 40 modules in ϕ in each disk) where it is read from the bias resistor side, and of the third ring in the TID (240 single modules) where it is read from the opposite side.

The angular pitch is $\phi = 0.01799°$ and the inner radius of the active region, is 392100 μm.
On the implant (metal) layer, the strip is large 31 (41) μm on the bias resistor side and 39 (51) μm on the opposite side. Only in this sensor, among the ones produced by HPK, the insertion of the shorter resistor type (R_1) was possible, due to the larger linear pitch of the strips.
DC and AC pads on both sides are positioned at a constant step along all the sensor width, as shown on Fig.10. On the top side, the DC pads and the first row of AC pads are exactly aligned on the vertical axis to allow an easier testing procedure. All the strips are numbered on both sides.
The W3 mini-sensor has 64 strips, for an active lenght of 50000 μm.

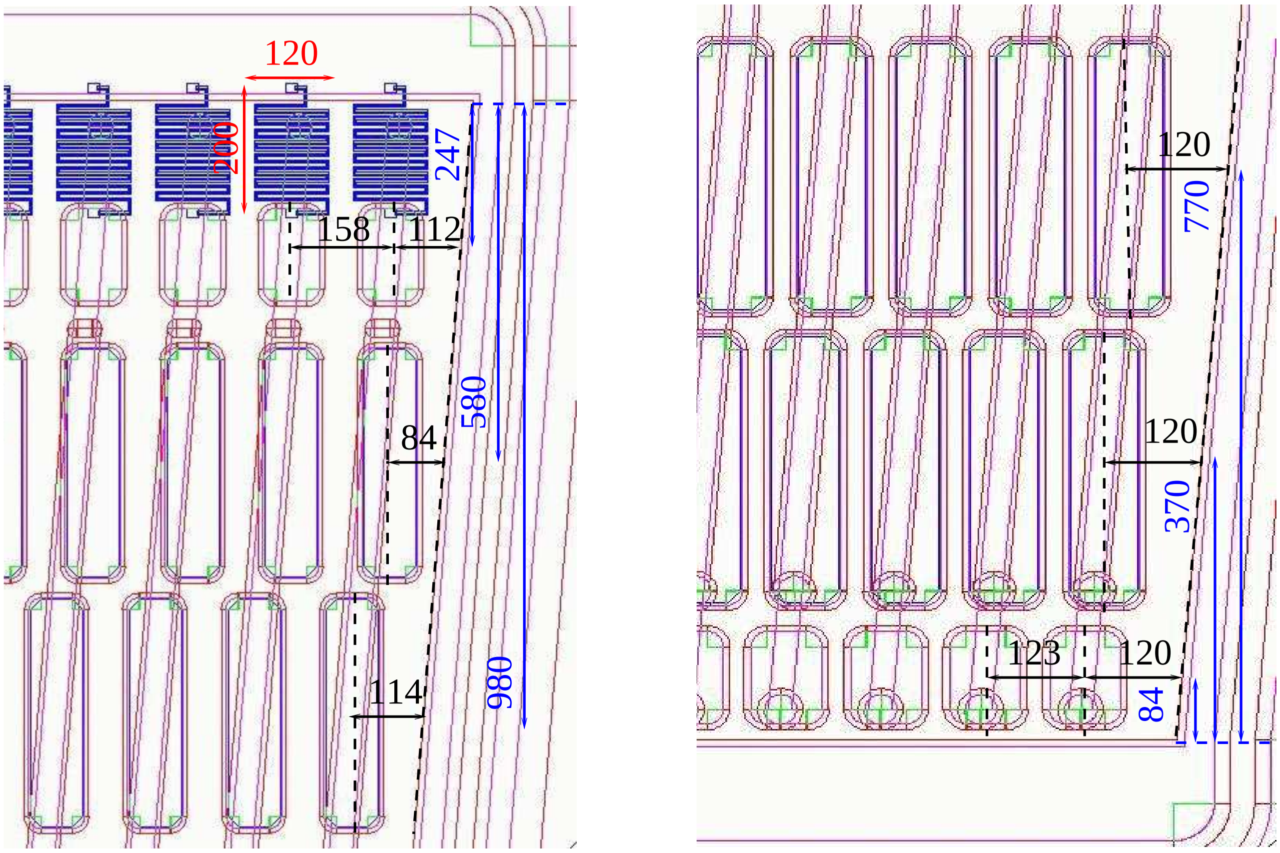

Figure 10: Views of the edges of the active region on the two opposite sides of the W3 detector.

- **W4:** This wedge detector, made of 512 strips, is the sensitive element of the fourth ring in the TEC (1008 single modules, 56 modules in ϕ in

each disk) where it is read from the bias resistor side.
The inner radius of the active region is at 504100 μm and the angular pitch is $\phi = 0.012856°$.
On the implant (metal) layer, the strip is large 35 (45) μm on the bias resistor side and 28 (36) μm on the opposite side.
DC and AC pads are positioned following the same criteria as in the W3 detector (see Fig.11). The W4 mini-sensor has 128 strips, for an active lenght of 80000 μm.

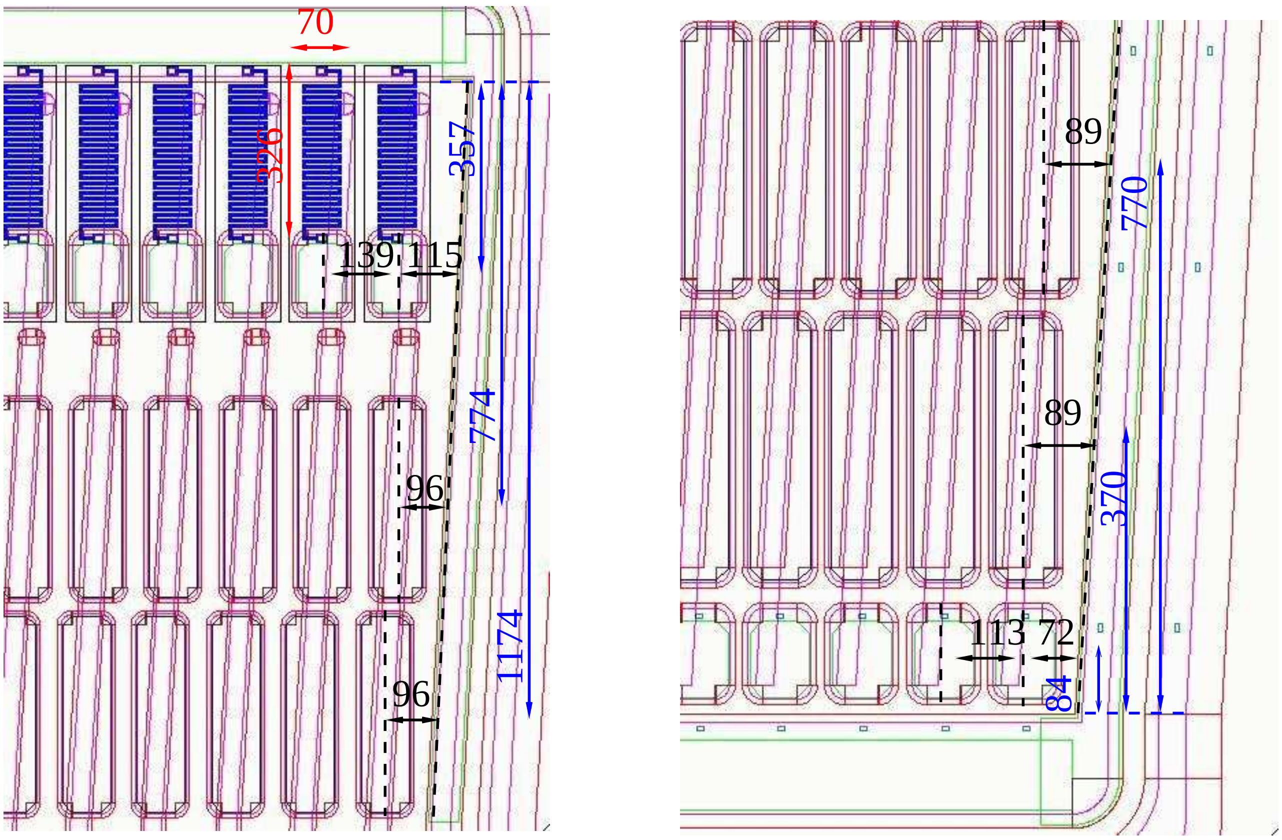

Figure 11: Views of the edges of the active region on the two opposite sides of the W4 detector.

6 STM Silicon Sensors

- **Wafer layout:** Thick sensors foreseen for the CMS silicon tracker are produced by STMicroelectronics (Catania, Italy). Each wafer contains a large area sensor located inside a circular region of approximately 13.95 cm diameter, where the process is guaranteed.

The available space surrounding the main sensors is filled with additional structures: the standard half-moon, MOS devices and diodes, a mini-sensor and some specific structure required by the company for the process qualification. The typical design of a wafer is shown in figure 12.

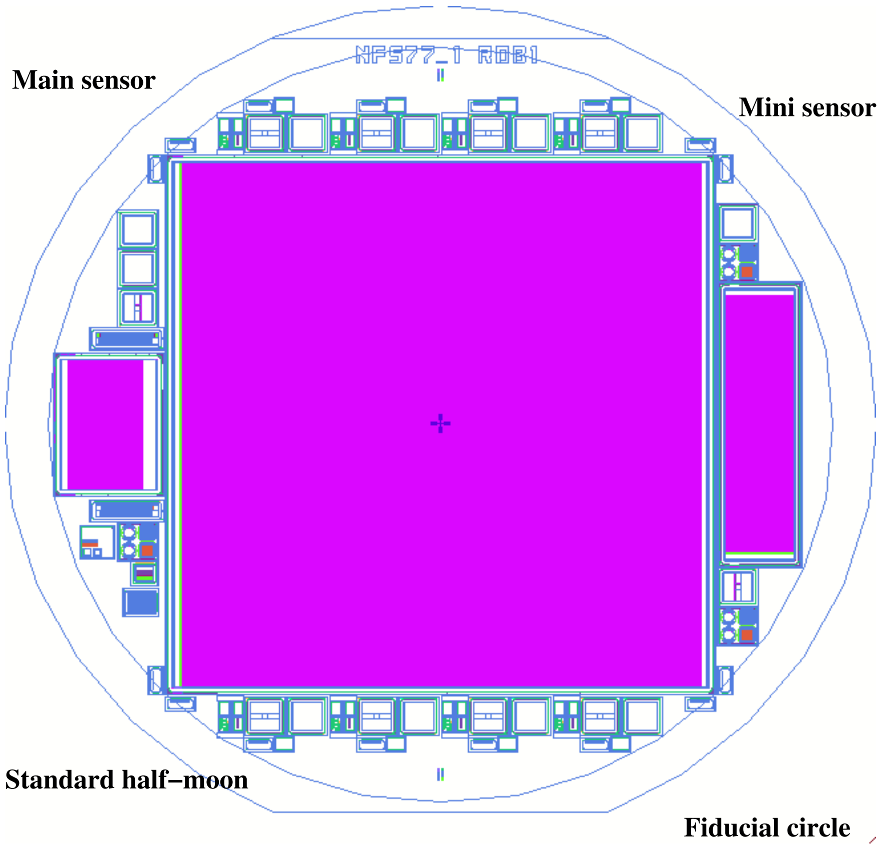

Figure 12: Mask design for Outer Barrel (OB1) sensors.

- **Strip structure:** The p^{+} implant and the metal layer of the strips are designed following the rules described in section 2.
  The edges of the strip have rounded corners in implant and metal layers to avoid critical electrical fields.
  Strips are AC-coupled through an array of capacitors made of a multilayer of thin dielectrics.
  The strips are biased via resistors connected to the bias ring. Resistors are made of a poly-silicon deposition with a wiggle-shaped structure. Each resistor is 100 μm wide, 300 μm long and consists of 665 polysilicon squares phosphorus doped. All resistors are positioned on one

end of the strip to allow for easier testing procedures.
One row of DC pads and two rows of AC pads are present on each detector side and are aligned orthogonally to the strip direction. A common feature for the pad design is the use of 6 μm metal over-hang and a contactable region 1 μm wider than the p^+ implant.
The width of the pads is designed as large as possible accordingly with the strip pitch. As a consequence, the dimensions of the pads depend on the sensor design. The values chosen for each detector type are indicated in the sketches included in this note. The optimization of the AC pad design includes the use of a thicker oxide layer under the pad to reduce the probability of damaging the capacitor during the testing and the bonding.
The DC pads are designed as close as possible to the bias ring. The distance between the p^+ implant of the DC pad and the bias ring in the side perpendicular to the strip direction is 29 μm where poly-silicon resistors are not included and 433 μm in the side where resistors are designed. The distance between the first and last strip and the bias ring on the side along the strip direction depends on the sensor type.
The distance between the DC and the first AC pads, along the strip, is 20 μm and the second AC pad is designed at a distance of 38 μm.

- **Bias and Guard ring:** The sensors produced by STMicroelectronics have the same structure for the bias and guard ring.
  Both rings have an asymmetrical design since the side perpendicular to the strip direction is wider than the parallel one. This geometry is required to simplify the micro-bonding and the testing operation.
  The layout of bias and guard ring is shown in fig. 13.

  Each ring is metallised with an aluminium deposition. The bias ring has a metal over-hang only in the external side, while a metal deposition wider than the p^+ implant is designed on both sides of the guard ring.
  The passivation layer is opened on the larger side of both rings and along the side parallel to the strip direction up to the second row of AC pads.
  A detailed description of the geometry for bias and guard ring is reported in Table 7.

- **Structure of the detector non-sensitive region:** The design of the edge region is the same for all sensors type. A schematic view is shown in figure 14.

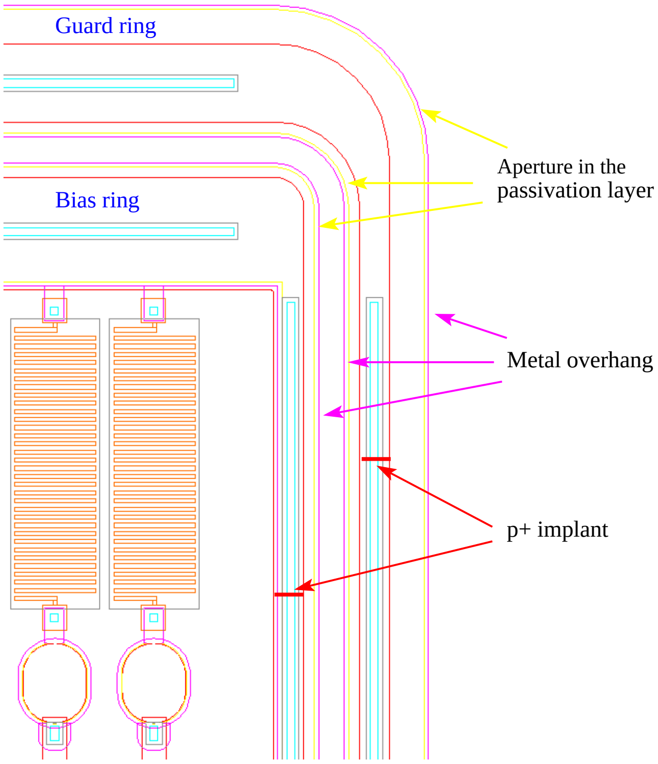

Figure 13: Structure of bias and guard ring for sensors produced by STMicroelectronics.

	Implant width	Metal over-hang on the internal side	Metal over-hang on the external side
Bias ring (side perpendicular to the strip direction)	138	-5	18
Bias ring (side along the strip direction)	37	-5	18
Guard ring (side perpendicular to the strip direction)	96	18	48
Guard ring (side along the strip direction)	37	18	48

Table 7: Dimensions of the p^+ implant and metal layer for the bias and guard ring.

The n^+ implant is designed at a distance of 700 μm from the external edge of the p^+ implant on the guard ring. In the internal side of n^+ implant 50 μm metal over-hang is implemented.
The width of the n^+ region is 410 μm for all the rectangular detector sides. Wedge sensors have a variable width in the side parallel to the strip direction.
The distance between the active area, i.e. the internal edge of p^+ implant of the bias ring, and the cutting edge is 1410 μm along the strip direction and 1250 μm orthogonal to the strip direction. For the wedge sensors the distance along the strip direction depends on the sensor design.
In order to protect the sensor, the whole area is covered with a layer of silicon oxide. Neverthless the passivation layer is opened along the strip direction close to the row of poly-silicon resistors and in the region where the contact is needed.
An identification code is inserted along the strip direction close to the side where poly-silicon resistors are designed. It contains information regarding the company, the sensor design, the batch and sensor number.
The strips are numbered on both the sides perpendicular to the strip direction. Numbers are defined using a metal layer over the n^+ implant in a region where the aluminium is not deposited. For each side only even or odd strips are indicated. Strips are numbered from left to right if the side with resistors is in the upper part of the sensor.
The alignment of detectors for module construction is allowed by a suitable marker shown in figure 14. The L-shaped marker is designed as an opening inside the metal layer over the n^+ implant. Each side is 800 μm long and 200 μm wide. The circle inside the marker has a diameter of 100 μm and each cross reference has a lenght of 47 μm and a width of 15 μm. The circular mark has been designed at 260 μm from the external edge of the metal layer.
The sensors will be diced by the company with a tolerance of $\pm 20\mu$m. The precision of the dicing has been improved using a square mark located in the detector corners. The contrast between different zones, shown in the figure, is clearly visible with a microscope and allows to define in a precise way the edge of the cutting line.

6.1 Review of the characteristics of STMicroelectronics sensor types

Different designs are defined for thick sensors: two for the rectangular detectors and six for the wedge ones.

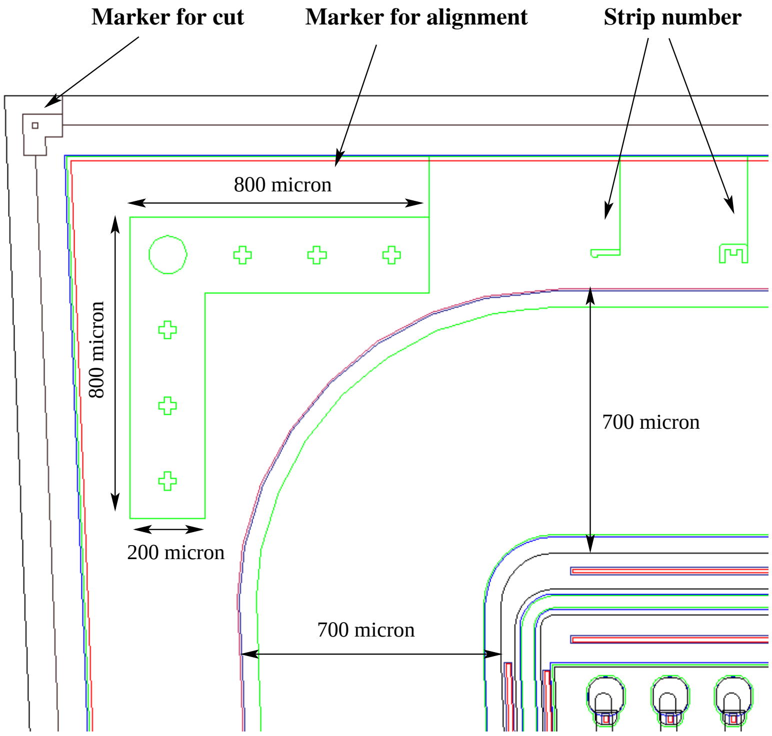

Figure 14: External region of STMicroelectronics sensors.

Rectangular sensors, designed for the outer barrel module (TOB), have parallel strips with a constant linear pitch.
Wedge detectors, designed for the endcap region of the Tracker (TEC), have radial strips with a constant angular pitch. The pitch for DC and AC pads is chosen as the mean value of the distance between two adjacent strips. DC and AC pads have been aligned wherever it was possible.
The thick modules designed for the TEC (ring 5, 6 and 7) consist of two sensors having the read-out strips daisy-chained electrically connected with microbonding wires. For each ring two sensor mask, named A and B, have been designed with the same angular strip pitch for the main sensor. The mini-sensor included in the wafer layout for sensor A and B of each ring is identical. It has been designed with the pad position and strip pitch as the read-out side of the corresponding wedge module.
A detailed geometrical description of each sensor is presented in the sketches at the end of the document.
The characteristics of each sensor design are discussed in the following.

- **OB1:** OB1 is a rectangular detector used to build the outer barrel modules of the CMS tracker.

It has 768 strips with a constant pitch of 122 μm. The mini-sensor has 96 strips and an active area of $11890 \times 50000 \mu m^2$.
Total number of OB1 sensors is 5520. These detectors are required for the r-ϕ side of 1080 double-sided modules of the first two layers of the TOB and for 1680 single-sided module that will be installed on the layer 5 and 6.

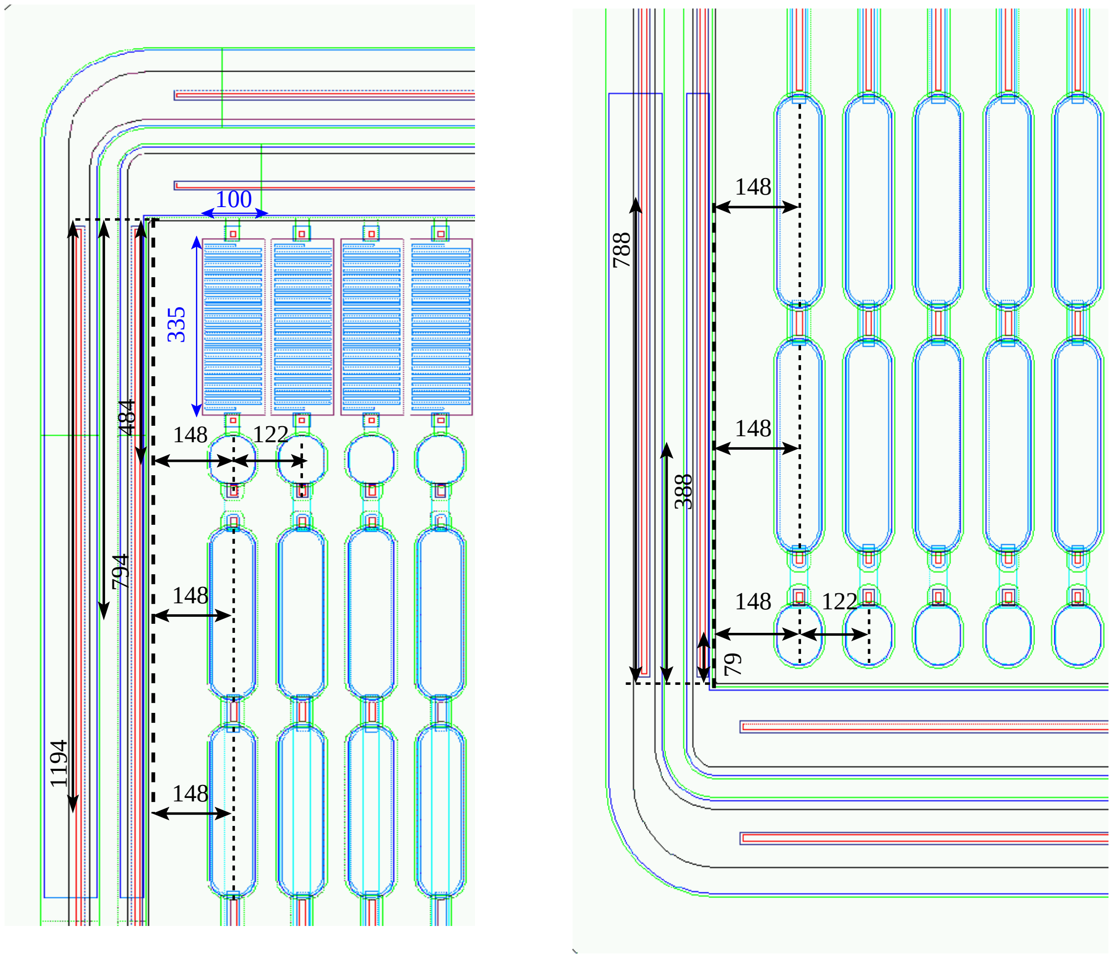

Figure 15: Top (a) and bottom (b) left corner of OB1 sensor. Distances between DC and AC pads and bias ring are indicated.

- **OB2:** The second design for outer barrel sensors has the same sensitive area of OB1 detectors, but the number of strips is 512 and the pitch is 183 μm.
  The mini-sensor consists of 64 strips and has an active area of $48058 \times 50000 \mu$m.

These sensors will be used to build the stereo side of 1080 double-sided modules for the first two layers of the TOB and 1368 single-sided modules to equip the third and fourth layers.

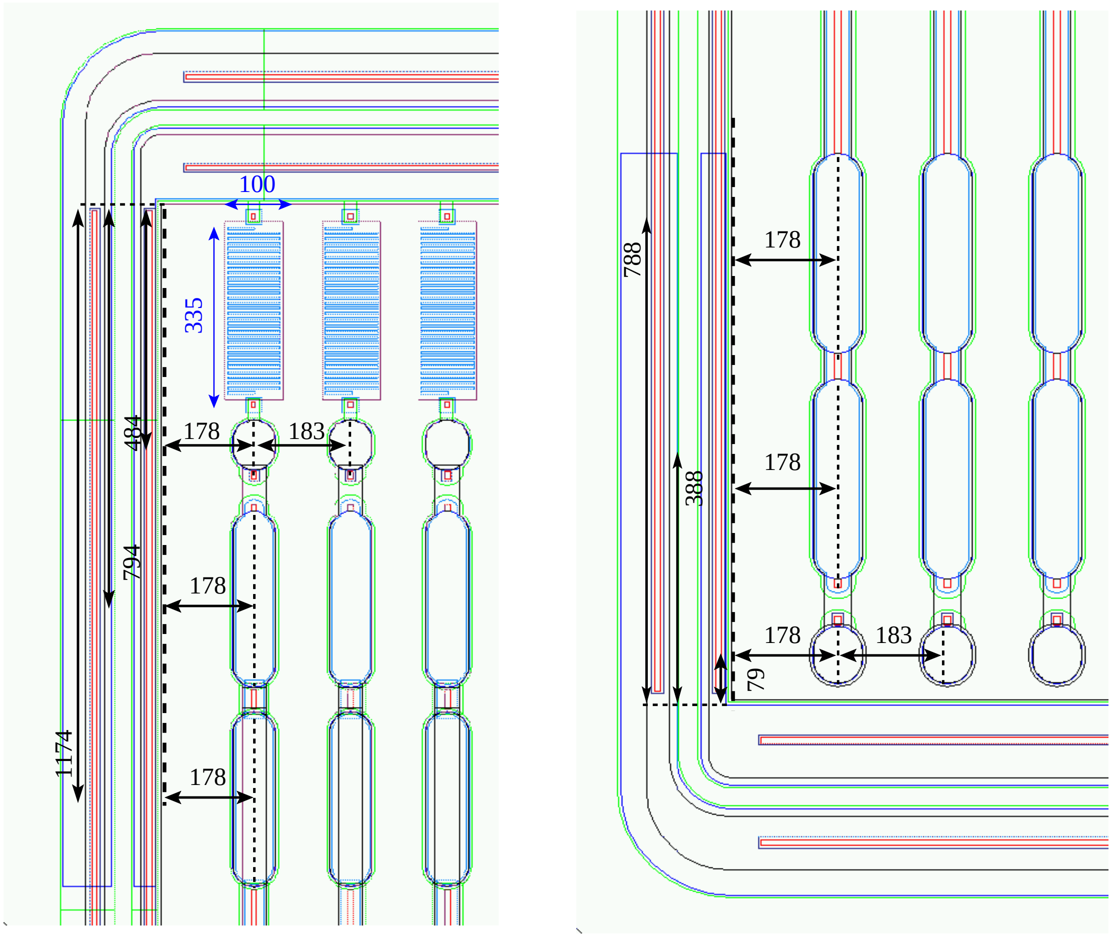

Figure 16: Bottom (a) and top (b) left corner of OB2 sensor. Distances between DC and AC pads and bias ring are indicated.

- **W5 - sensor A:** W5A sensors will be used to build modules for the fifth ring of the TEC. The radius of the active area, i.e. the internal edge of the bias ring, is 603200 μm. Radial strips are designed with a constant angular pitch $\phi = 0.011909$ degrees.
  The distance between the pads on the first (and last) strip and the bias ring is not constant. Fig 17 shows the corners (top and bottom) of the sensor and the mean distance for DC and AC pads.

  W5A sensors will be assembled with the W5B sensors and the read-out electronics will be placed on the larger side of W5B.

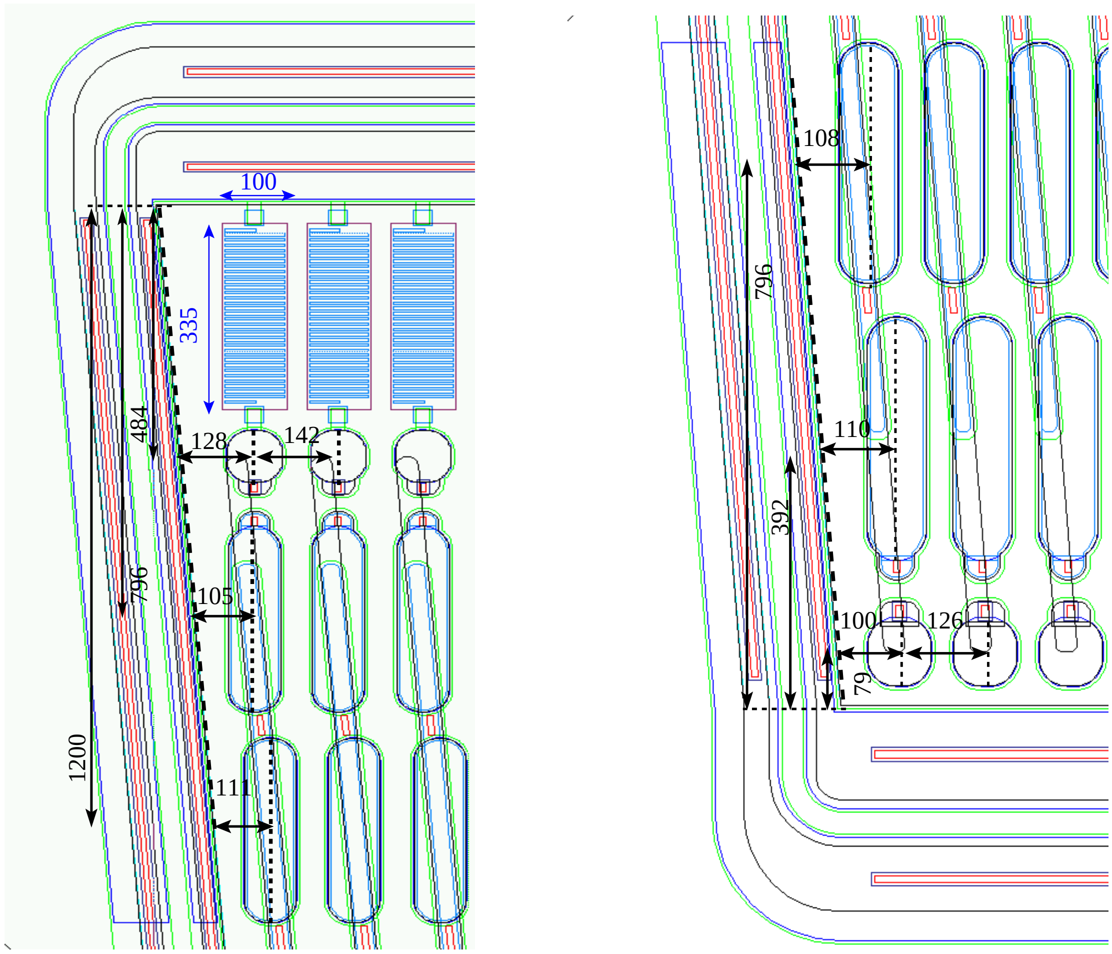

Figure 17: Bottom (a) and top (b) left corner of W5A sensor. Distances between DC and AC pads and bias ring are indicated.

The mini-sensor has the same strip pitch of the module read-out side. It has 64 strips and an active area 50000 μm long.

- **W5 - sensor B:** The angular pitch for W5B is $\phi = 0.011909$ degrees. The radius of the active area is 687293 μm.
  Design of angle with mean distance from pad to bias ring.
  The mini-sensor on W5B is identical to the one designed in the W5A mask and has the same radial geometry of the W5B read-out side.

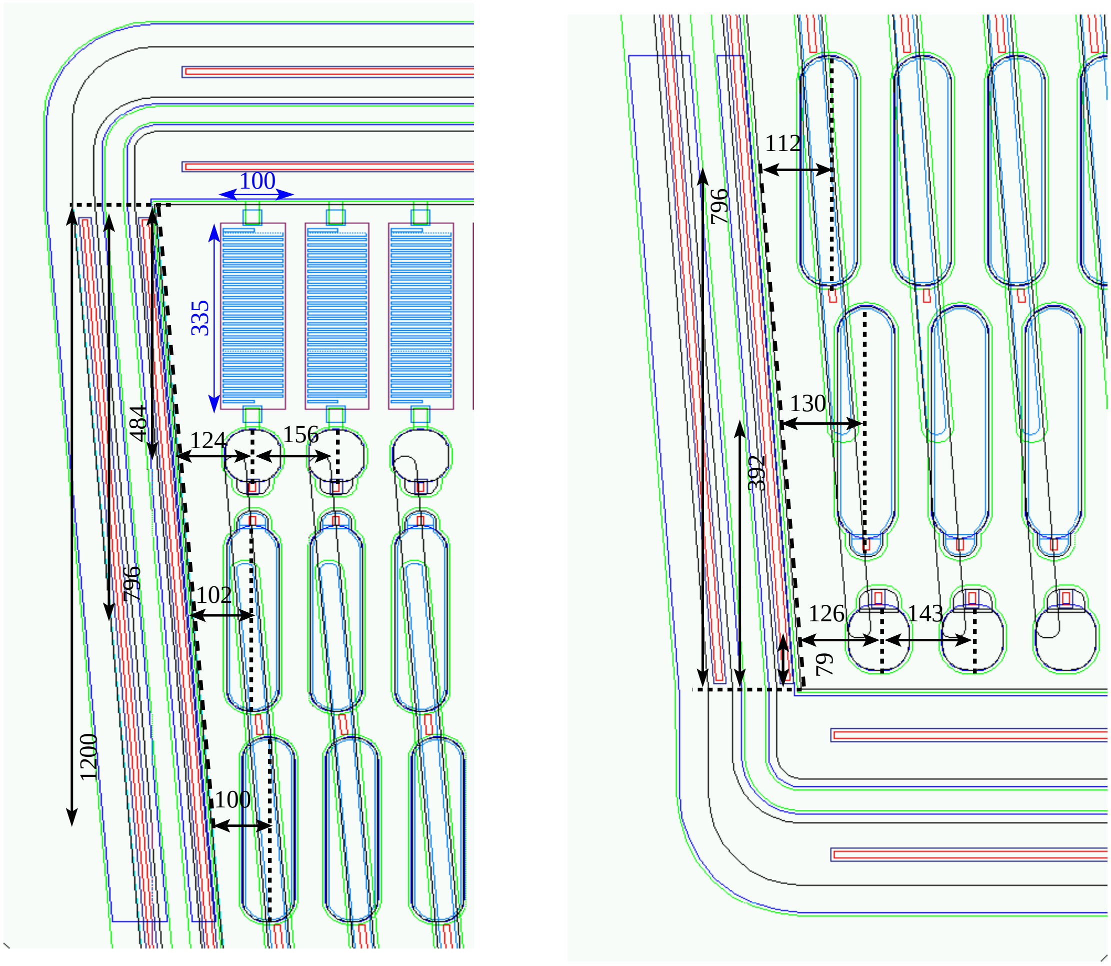

Figure 18: Bottom (a) and top (b) left corner of W5B sensor. Distances between DC and AC pads and bias ring are indicated.

- **W6 - sensor A:** The angular pitch for W6A is $\phi = 0.012847$ degrees. The radius of the active area, i.e. the internal edge of the bias ring, is 727000 μm.

Design of angle with mean distance from pad to bias ring.
W6A sensors will be daisy-chained with the W6B sensors and the read-out electronics will be placed on the larger side of W6B.
The mini-sensor has 64 strips and an active area of 50000 μm long. The pad position on the read-out side have the same pitch of the W6B larger side.

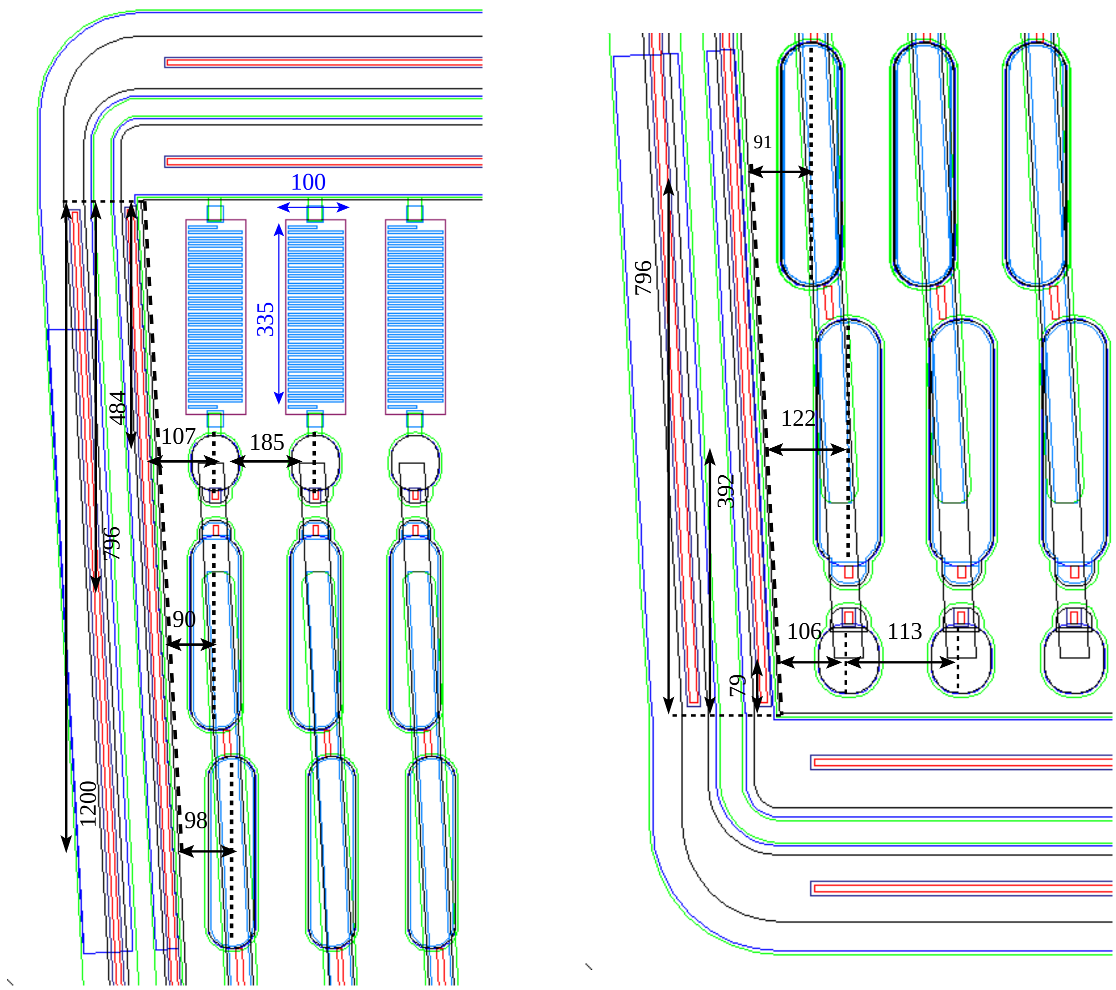

Figure 19: Bottom (a) and top (b) left corner of W6A sensor. Distances between DC and AC pads and bias ring are indicated.

- **W6 - sensor B:** The angular pitch of W6B strips is $\phi = 0.012847$ degrees.
  The radius of the active area is 826060 μm.
  Design of angle with mean distance from pad to bias ring.

The mini-sensor on W6B is identical to the one designed in the W6A mask.

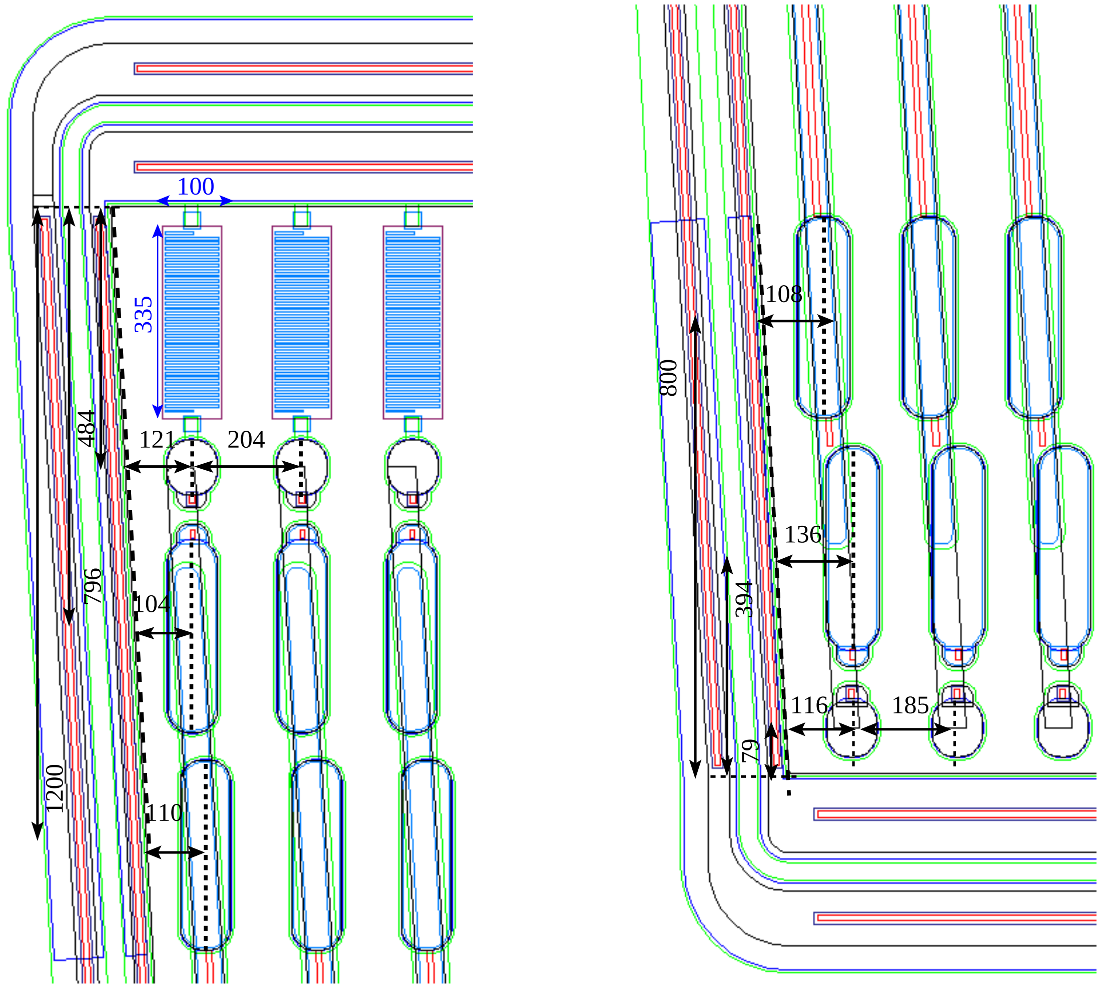

Figure 20: Bottom (a) and top (b) left corner of W6B sensor. Distances between DC and AC pads and bias ring are indicated.

- **W7 - sensor A:** The angular pitch for W7A is $\phi = 0.009$ degrees. The radius of the active area, i.e. the internal edge of the bias ring, is 888400 μm.
  Design of angle with mean distance from pad to bias ring.
  Main sensor has a different scheme for strip numbering. Strips are labelled from left to right, leaving the sensor with the resistor side on the lower part.

W7A sensors will be daisy-chained with the W7B sensors and the read-out electronics will be placed on the smaller side of W7A.
The mini-sensor has 64 strips and an active area of 50000 μm long.

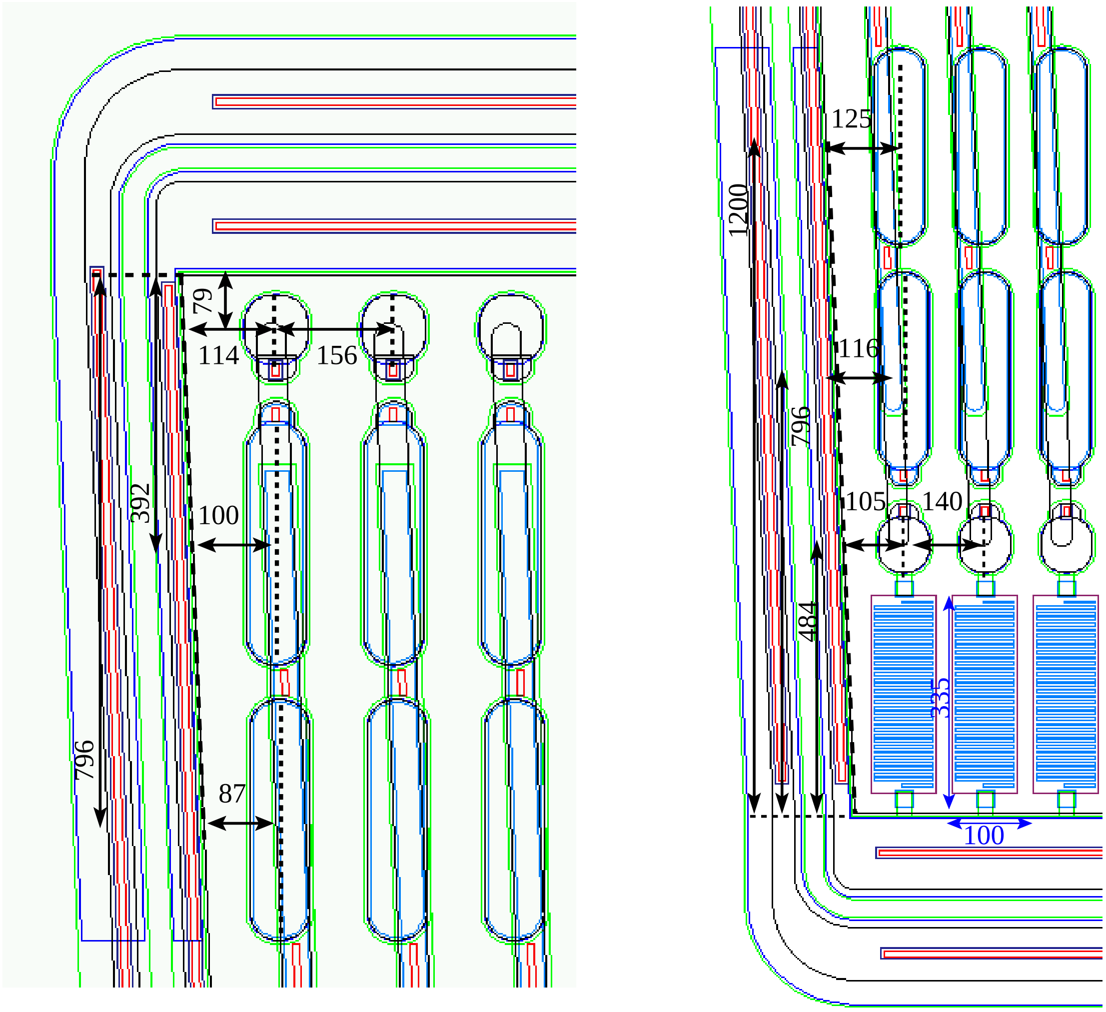

Figure 21: Bottom (a) and top (b) left corner of W7A sensor. Distances between DC and AC pads and bias ring are indicated.

- **W7 - sensor B:** The angular pitch for W7B is $\phi = 0.009$ degrees. The radius of the active area is 998252 μm.
  Design of angle with mean distance from pad to bias ring.
  Strips are numbered as in the W7A sensor.
  The mini-sensor on W7B is identical to the one designed in the W7A mask.

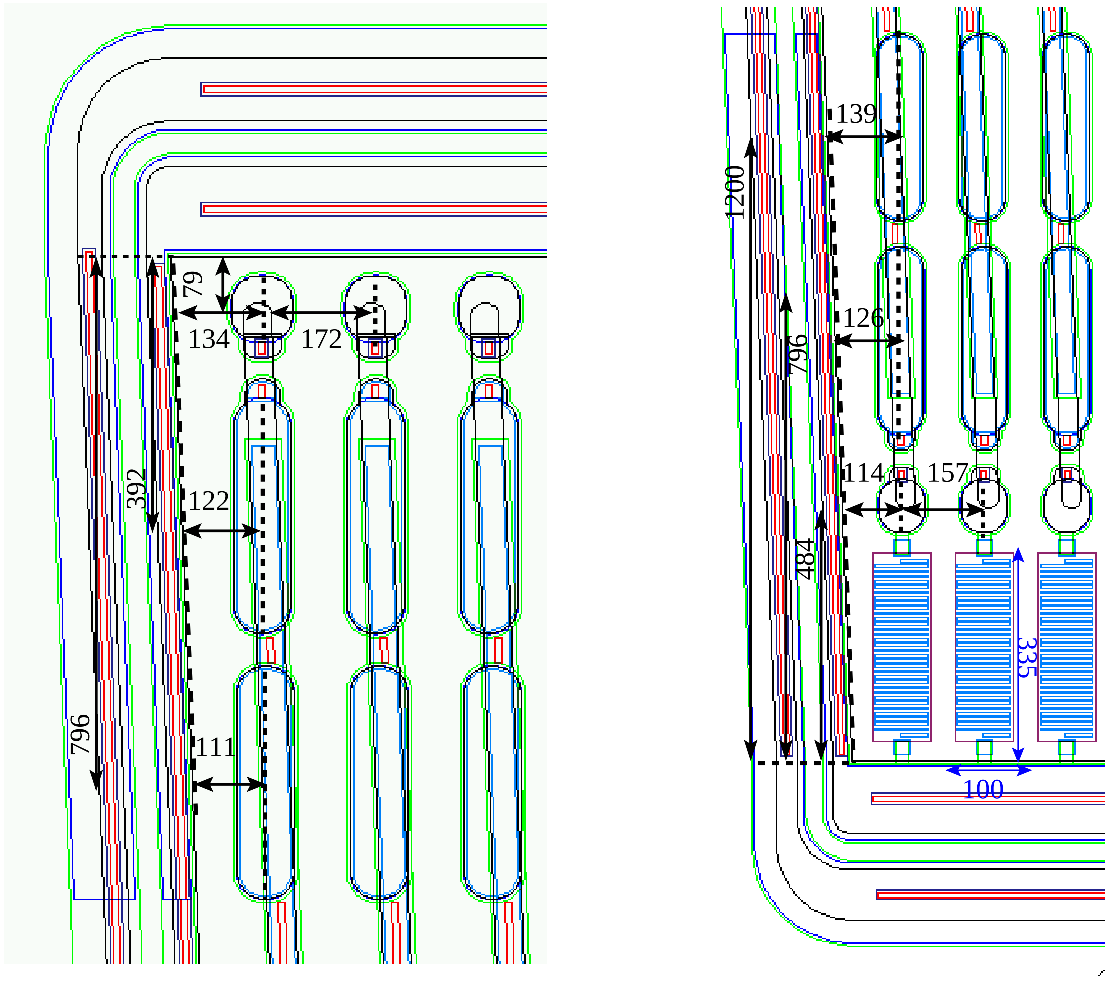

Figure 22: Bottom (a) and top (b) left corner of W7B sensor. Distances between DC and AC pads and bias ring are indicated.

Attention: dimensions on the sketch are all relative to the metal layer (except for the external cut-line)

Parameter	Value (μm)
Overall width (after cutting)	63328
Overall lenght (after cutting)	118961
Active area width	61540
Active area lenght	116885
Strip lenght	116825
Width of strip p+ zone	20
Pitch	80
Number of strips	768
Width of metal strip	28
Distance between end of strip's p+ zone and horizontal part of guard ring	30
Resistor height	326
Resistor width	70
Number of squares in a resistor	450
Bias pad height (aperture in passivation)	128
Bias pad width (aperture in passivation)	62
Bonding pad height (aperture in passivation)	364
Bonding pad width (aperture in passivation)	88
Width of the n zone between the edge of first guard ring p+ zone and n+ zone	300
Width of n+ zone	490

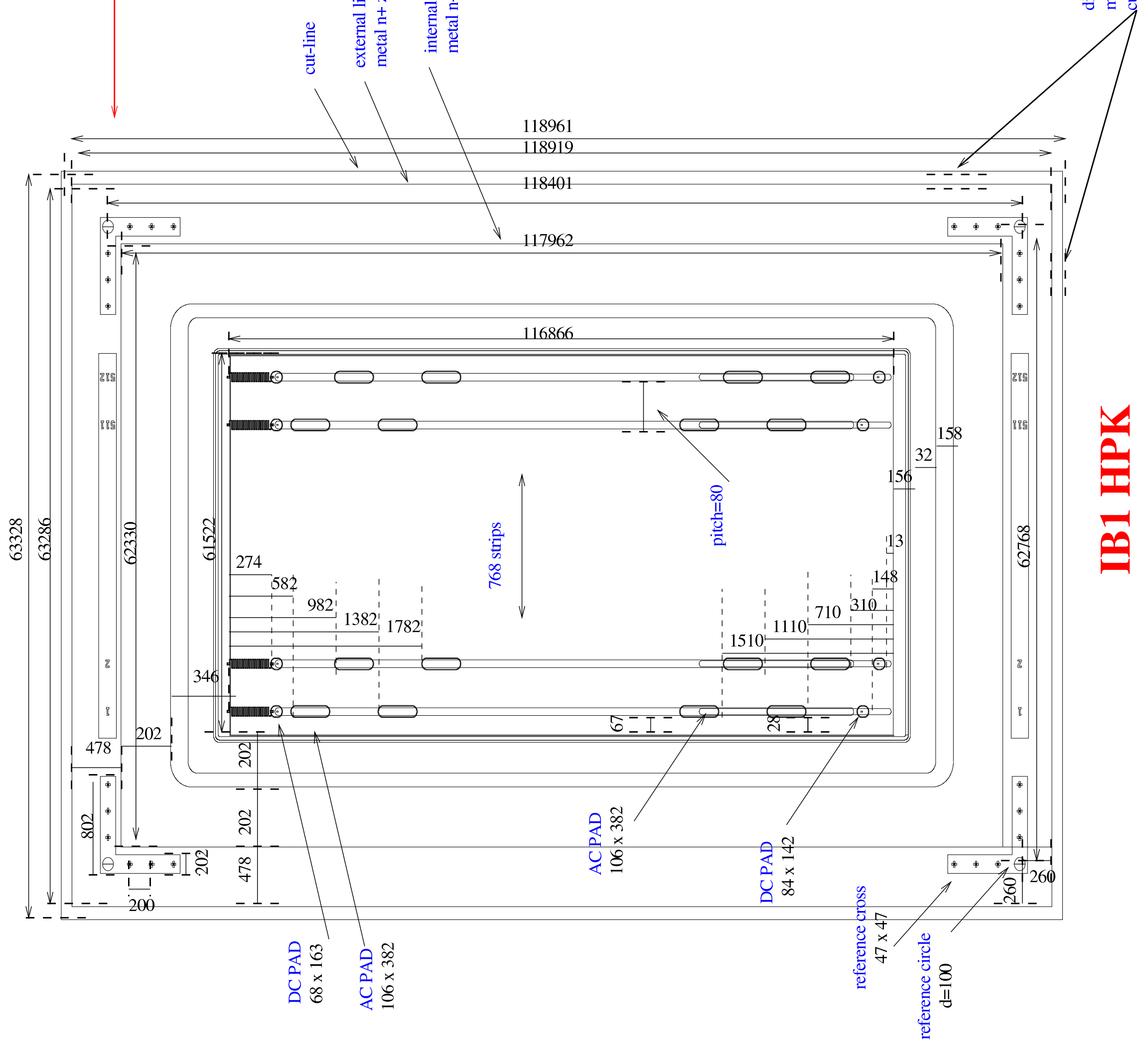

Figure 23: Schematics of the mask design for the IB1 detector

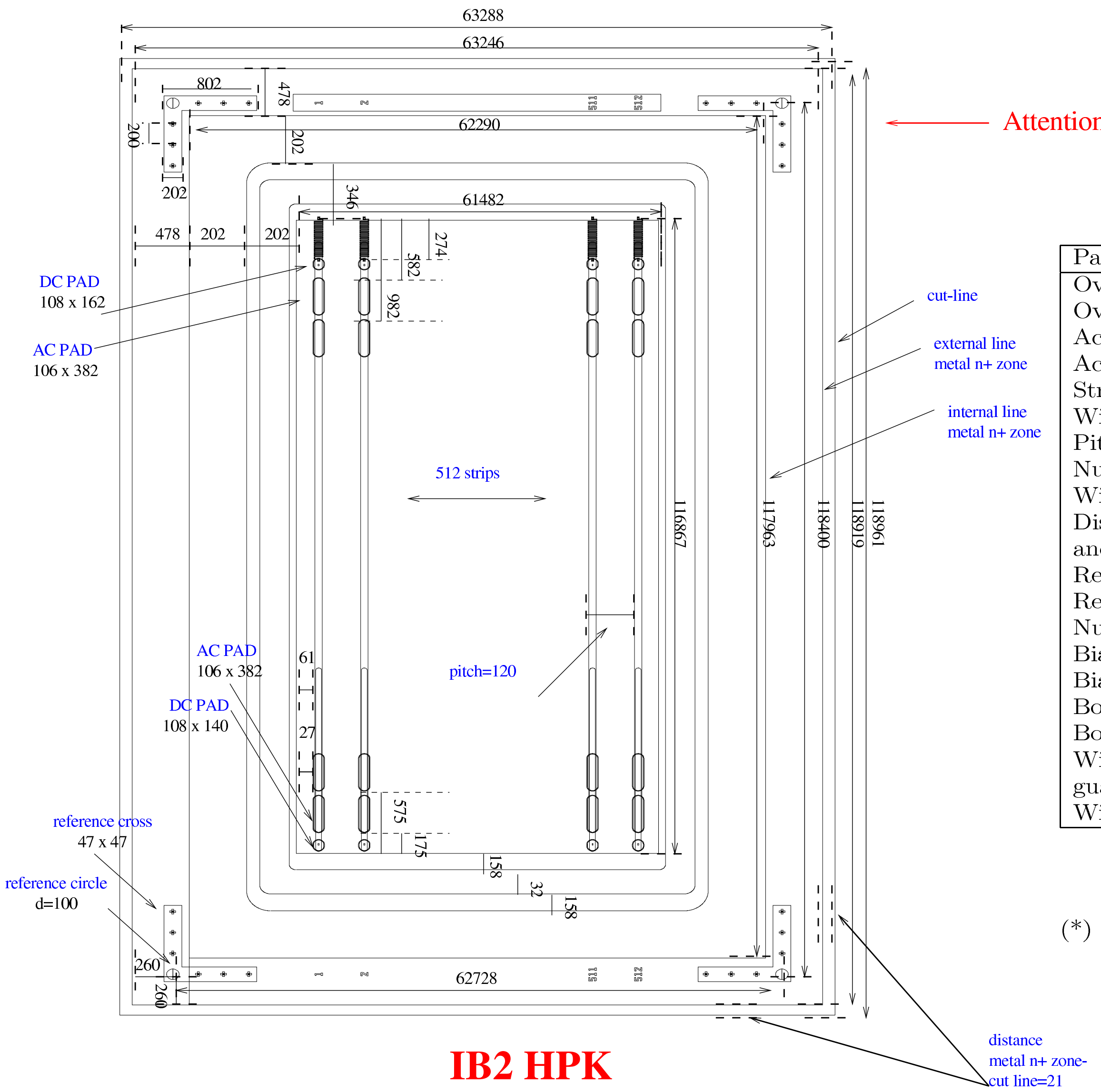

Attention: dimensions on the sketch are
all relative to the metal layer
(except for the external cut-line)

Parameter	Value (μm)
Overall width (after cutting)	63288
Overall lenght (after cutting)	118961
Active area width	61500
Active area lenght	116885
Strip lenght	116823
Width of strip p+ zone	30
Pitch	120
Number of strips	512
Width of metal strip	40
Distance between end of strip's p+ zone and horizontal part of guard ring	31
Resistor height	326
Resistor width	70
Number of squares in a resistor	450
Bias pad height(*)	128
Bias pad width (*)	88
Bonding pad height (*)	360
Bonding pad width (*)	88
Width of the n zone between the edge of first guard ring p+ zone and n+ zone	250
Width of n+ zone	450

(*) dimension of the aperture in the passivation layer

Figure 24: Schematics of the mask design for the IB2 detector

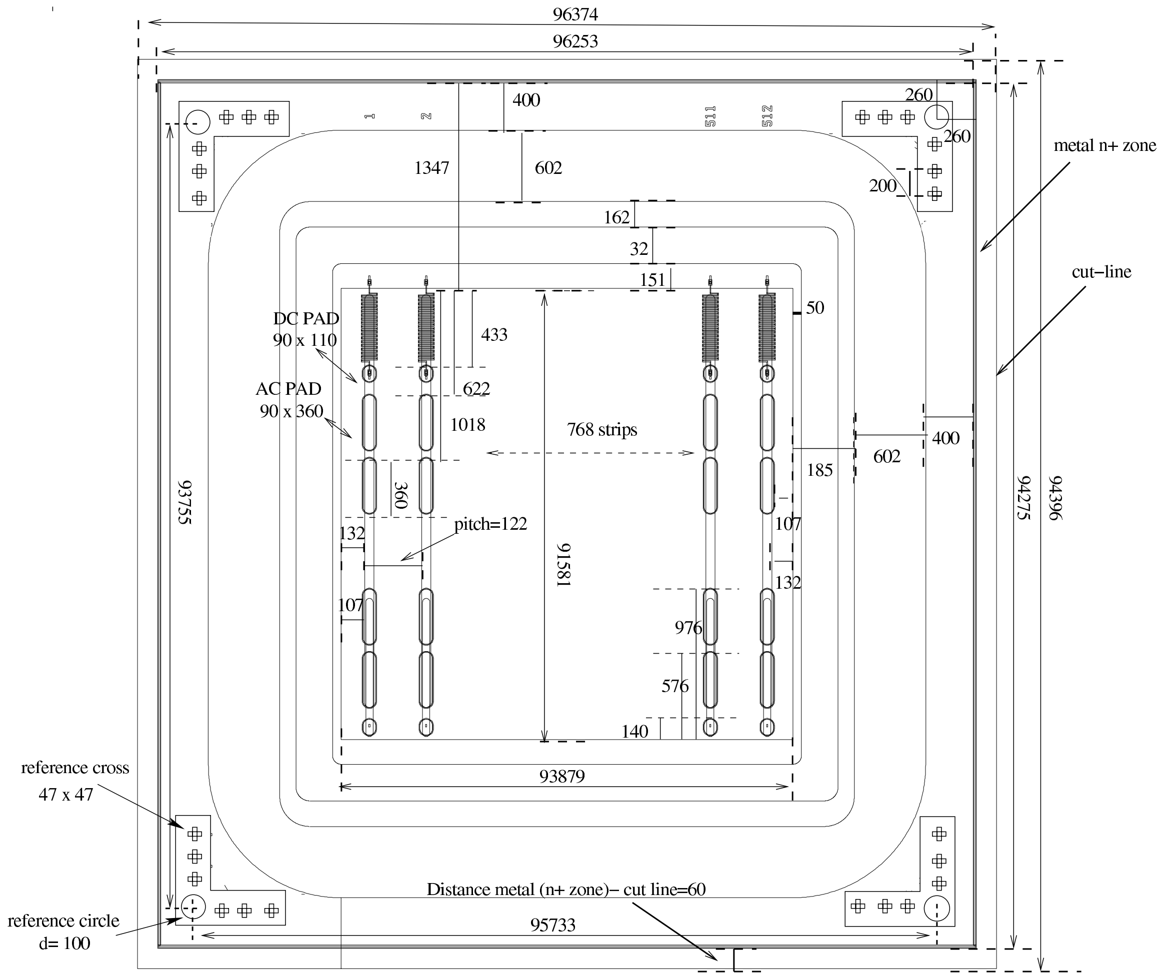

OB1

Dimensions in the sketch are referred to the metal layer (except for the external line)

Parameter	Value (μm)
Overall widht (after cutting)	96374
Overall lenght (after cutting)	94396
Active area width	93869
Active area lenght	91571
Strip lenght	91108
Width of strip p^+ zone	30
Pitch	122
Number of strips	768
Width of metal strip	40
Distance between end of strip p^+ zone and horizontal part of bias ring (lower side)	29
Distance between end of strip p^+ zone and horizontal part of bias ring (upper side)	433
Bias pad height (∗)	100
Bias pad width (∗)	80
Bonding pad height (∗)	350
Bonding pad width (∗)	80
Distance between the edge of guard ring p^+ zone and n^+ zone	700
Width of the n^+ zone	410

(*) Dimensions are referred to the opening in the passivation layer

Figure 25: Schematics of the mask design for the OB1 detector

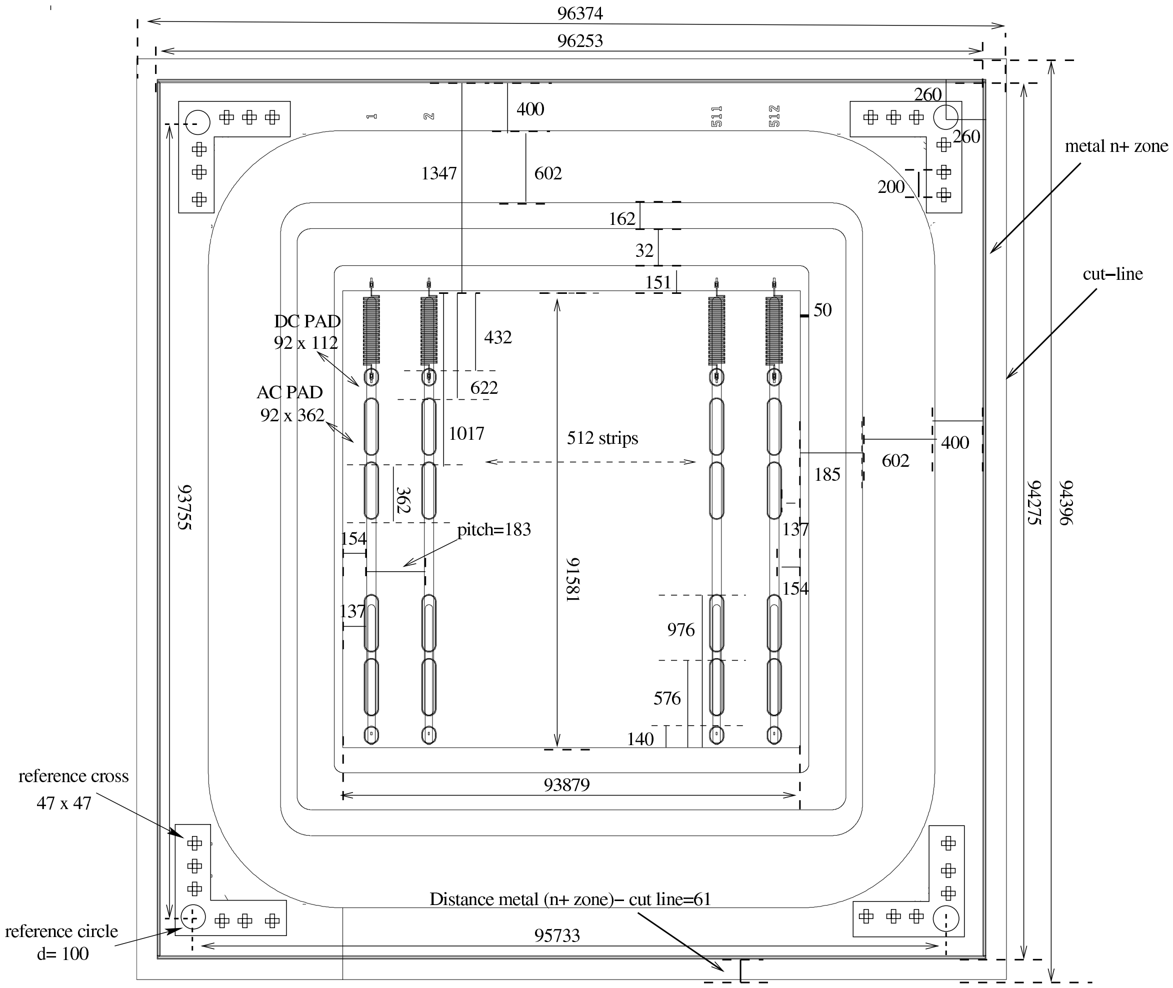

Figure 26: Schematics of the mask design for the OB2 detector

OB2

Dimensions in the sketch are referred to the metal layer (except for the external line)

Parameter	**Value (μm)**
Overall widht (after cutting)	96374
Overall lenght (after cutting)	94396
Active area width	93869
Active area lenght	91571
Strip lenght	91108
Width of strip p^+ zone	46
Pitch	183
Number of strips	512
Width of metal strip	58
Distance between end of strip p^+ zone and horizontal part of bias ring (lower side)	29
Distance between end of strip p^+ zone and horizontal part of bias ring (upper side)	433
Bias pad height (∗)	102
Bias pad width (∗)	82
Bonding pad height (∗)	352
Bonding pad width (∗)	82
Distance between the edge of guard ring p^+ zone and n^+ zone	700
Width of the n^+ zone	410

(*) Dimensions are referred to the opening in the passivation layer

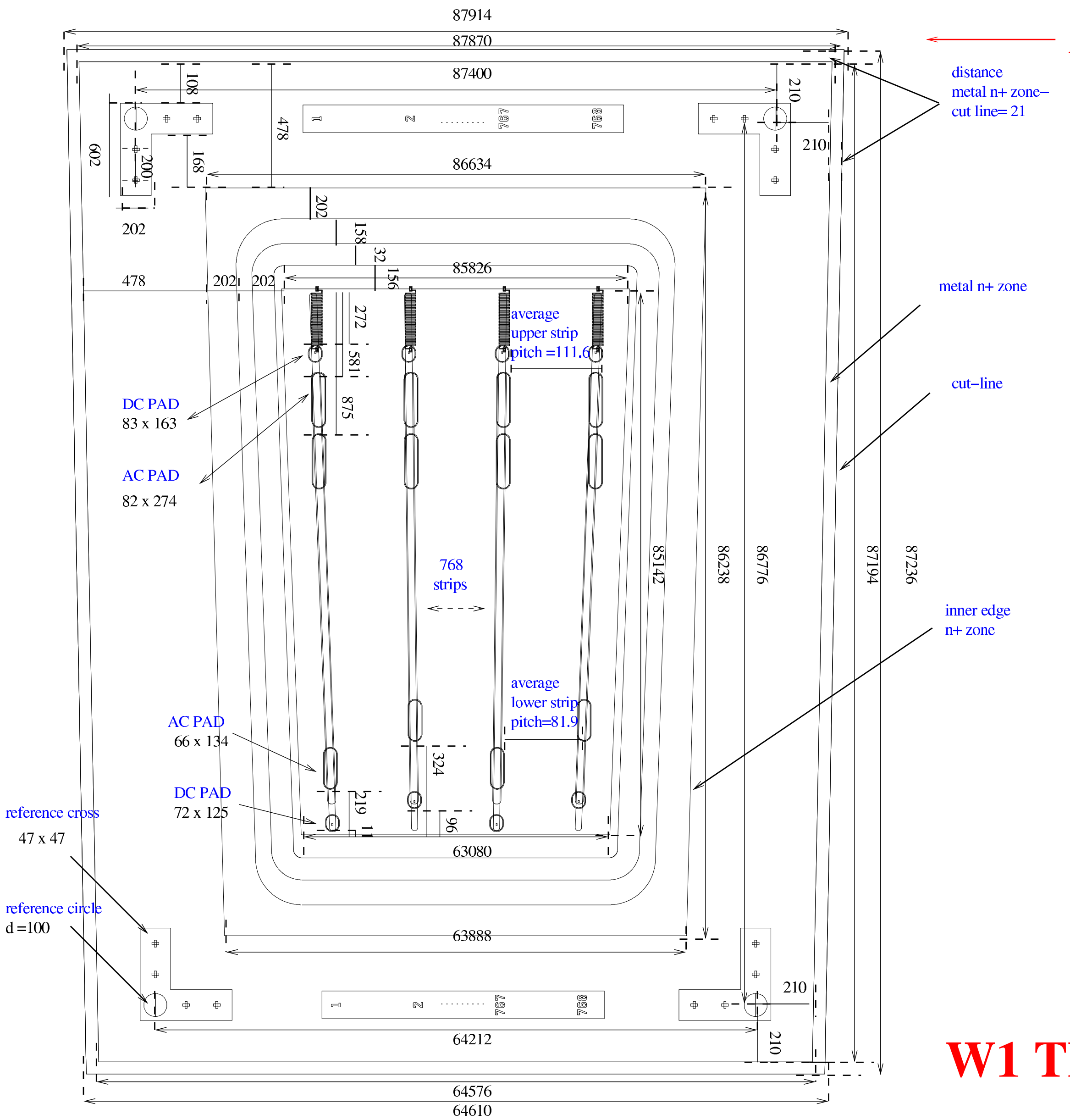

Attention: dimensions on the sketch are
all relative to the metal layer
(except for the external cut line)

Parameter	Value (μm)
Overall width (after cutting)	64610 –87914
Overall lenght (after cutting)	87236
Active area width	63100 – 85848
Active area lenght	85160
Strip lenght	85100
Width of strip p+ zone	20 –28
Average strip pitch	81.94 – 111.59
Number of strips	768
Width of metal strip	28 – 36
Distance between end of strip's p+ zone and horizontal part of guard ring	30
Resistor height	400
Resistor width	70
Number of squares in a resistor	450
Bias pad height, upper side (*)	128
Bias pad width, upper side (*)	62
Bonding pad height, upper side (*)	258
Bonding pad width, upper side (*)	65
Bias pad height, lower side (*)	90
Bias pad width, lower side (*)	66
Bonding pad height, lower side (*)	118
Bonding pad width, lower side (*)	50
Pitch for upper side bias pads (**)	111.60
Pitch for bonding pads, first upper row (**)	111.60
Pitch for bonding pads, second upper row (**)	111.33
Pitch for bias and bonding pads, lower row (**)	76.60
Width of the n zone between the edge of first guard ring p+ zone and n+ zone	300
Width of n+ zone	450

(*) aperture in the passivation layer
(**) Bias and bond pads have constant pitches but the first one in each group of 16 (8) in the upper (lower) side is adjusted to keep the contact with the corresponding strip.

W1 TEC HPK

Figure 27: Schematics of the mask design for the W1 TEC detector

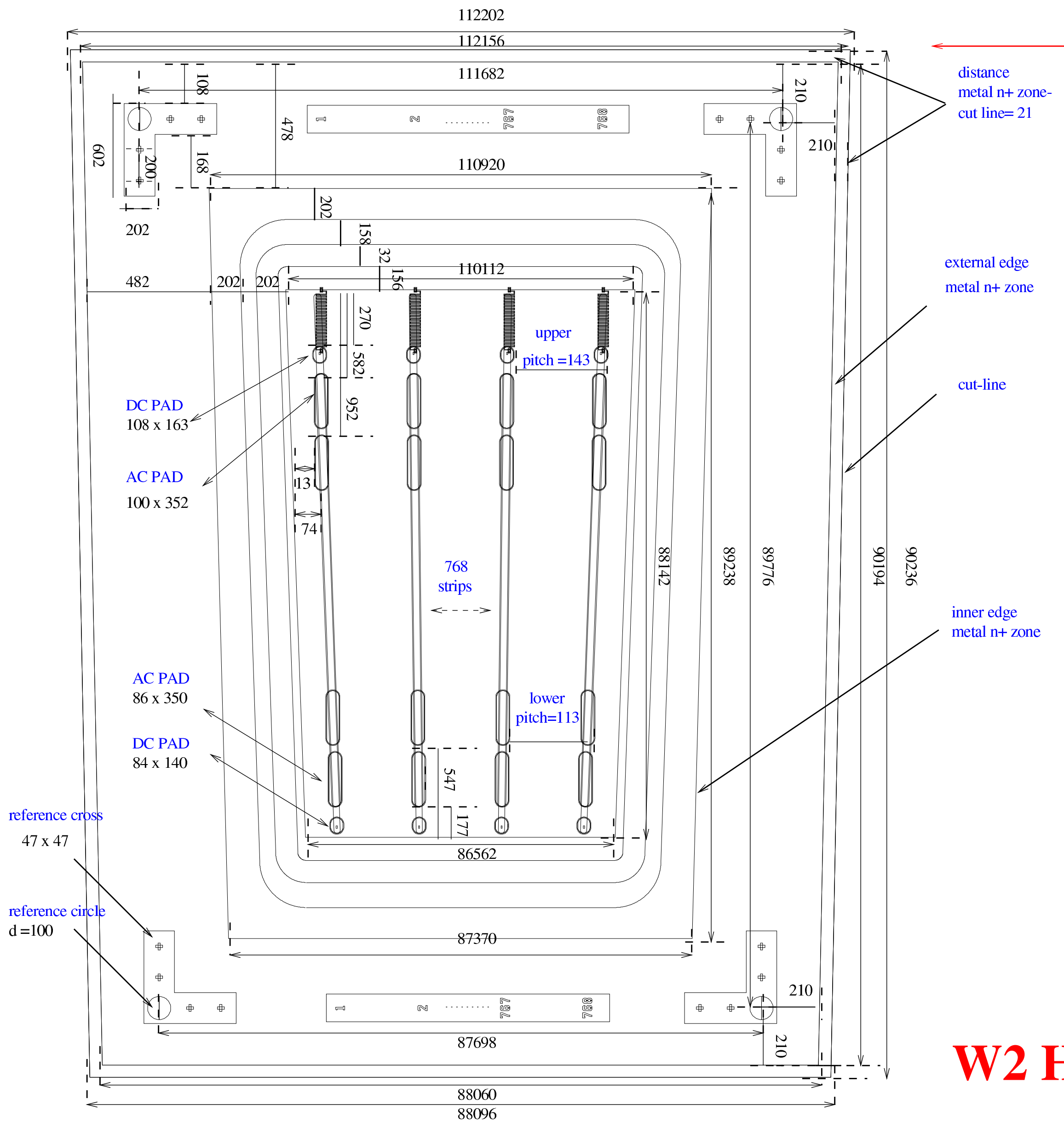

Parameter	Value (μm)
Overall width (after cutting)	88096 – 112202
Overall lenght (after cutting)	90236
Active area width	86580 – 110132
Active area lenght	88160
Strip lenght	88100
Width of strip p+ zone	28 – 36
Pitch	113 – 143
Number of strips	768
Width of metal strip	36 – 46
Distance between end of strip's p+ zone and horizontal part of guard ring	30
Resistor height	400
Resistor width	70
Number of squares in a resistor	450
Bias pad height, top (*)	128
Bias pad width, top (*)	88
Bonding pad height, top (*)	334
Bonding pad width, top (*)	82
Bias pad height, bottom (*)	104
Bias pad width, bottom (*)	64
Bonding pad height, bottom (*)	334
Bonding pad width, bottom (*)	70
Pitch for lower side bias pads (**)	112.77
Pitch for bonding pads, first lower row (**)	112.77
Pitch for bonding pads, second lower row (**)	112.77
Pitch for upper side bias pads (**)	142.97
Pitch for bonding pads, first upper row (**)	142.97
Pitch for bonding pads, second upper row (**)	142.90
Width of the n zone between the edge of first guard ring p+ zone and n+ zone	300
Width of n+ zone	450

(*) Aperture in the passivation layer
(**) Bias and bond pads have constant pitches but the first one in each group of 16 is adjusted to keep the contact with the relative strip.

W2 HPK

Figure 28: Schematics of the mask design for the W2 detector

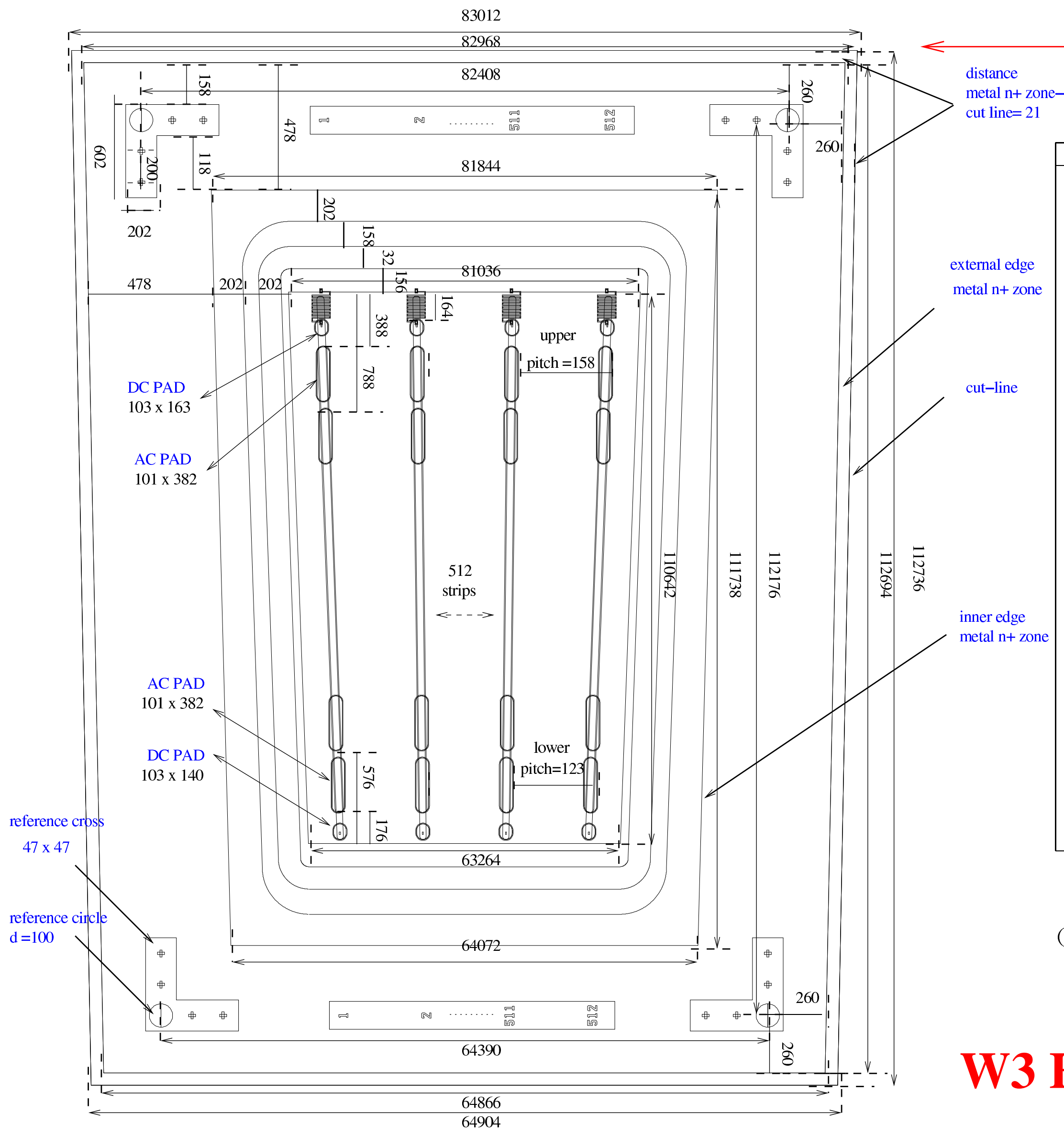

Parameter	Value (μm)
Overall width (after cutting)	64904 – 83012
Overall lenght (after cutting)	112736
Active area width	63282 – 81055
Active area lenght	110660
Strip lenght	110578
Width of strip p+ zone	31 – 39
Pitch	123 – 158
Number of strips	512
Width of metal strip	41 – 51
Distance between end of strip's p+ zone and horizontal part of guard ring	30
Resistor height	200
Resistor width	120
Number of squares in a resistor	450
Bias pad height, top (*)	128
Bias pad width, top (*)	83
Bonding pad height, top (*)	364
Bonding pad width, top (*)	83
Bias pad height, bottom (*)	105
Bias pad width, bottom (*)	83
Bonding pad height, bottom (*)	364
Bonding pad width, bottom (*)	83
Pitch for lower side bias pads	123.33
Pitch for bonding pads, first lower row	123.45
Pitch for bonding pads, second lower row	123.57
Pitch for upper side bias pads	158.06
Pitch for bonding pads, first upper row	158.06
Pitch for bonding pads, second upper row	157.83
Width of the n zone between the edge of first guard ring p+ zone and n+ zone	300
Width of n+ zone	450

(*) aperture in the passivation layer

Figure 29: Schematics of the mask design for the W3 detector

Attention: dimensions on the sketch are
all relative to the metal layer
(except for the external cut line)

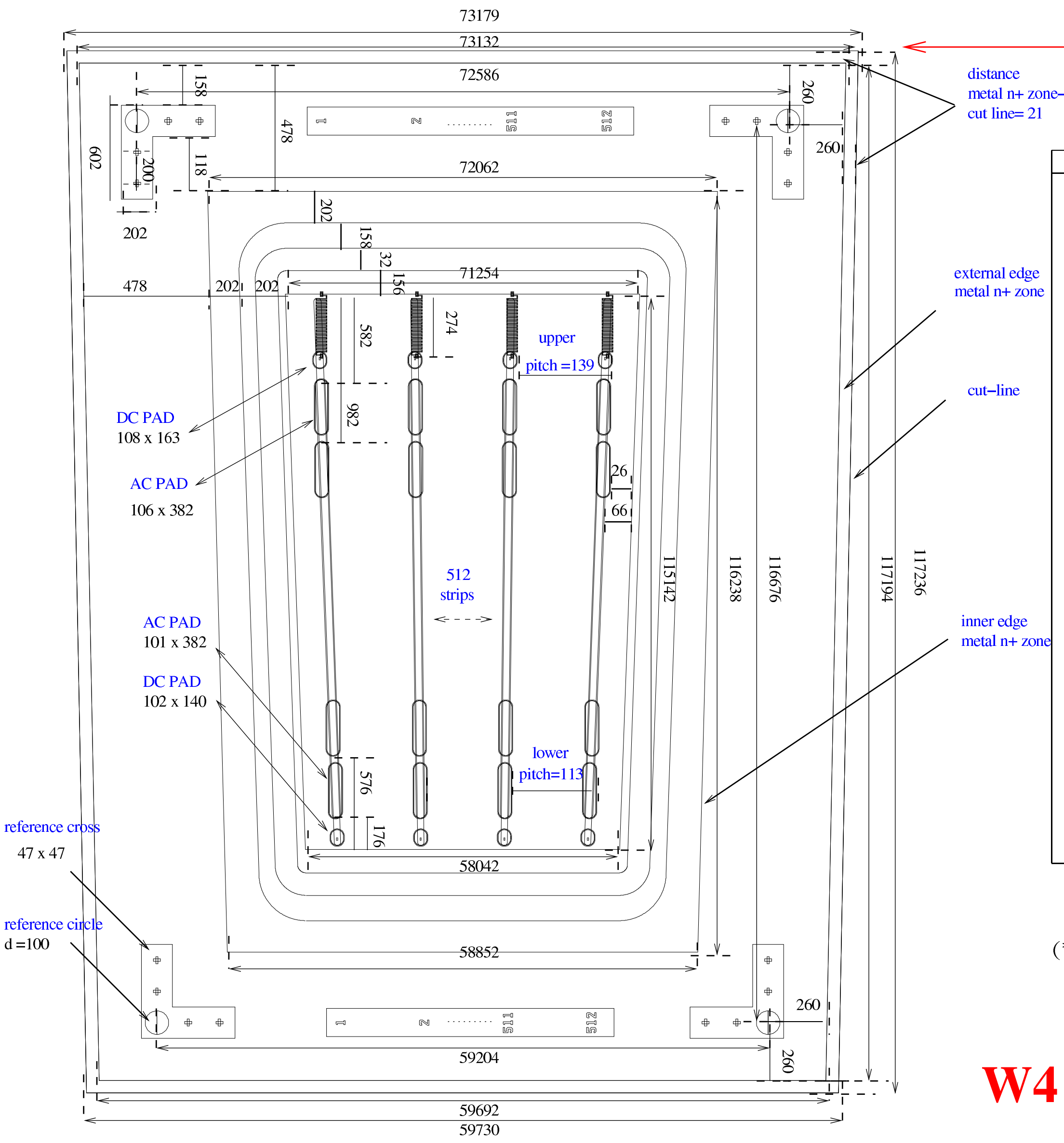

Parameter	Value (μm)
Overall width (after cutting)	59730 – 73179
Overall lenght (after cutting)	117236
Active area width	58060 – 71272
Active area lenght	115160
Strip lenght	115100
Width of strip p+ zone	28 – 35
Pitch	113 – 139
Number of strips	512
Width of metal strip	36 – 45
Distance between end of strip's p+ zone and horizontal part of guard ring	30
Resistor height	400
Resistor width	70
Number of squares in a resistor	450
Bias pad height, top (*)	128
Bias pad width, top (*)	88
Bonding pad height, top (*)	364
Bonding pad width, top (*)	88
Bias pad height, bottom (*)	105
Bias pad width, bottom (*)	81
Bonding pad height, bottom (*)	364
Bonding pad width, bottom (*)	83
Pitch for lower side bias pads	113.32
Pitch for bonding pads, first lower row	113.32
Pitch for bonding pads, second lower row	113.41
Pitch for upper side bias pads	138.92
Pitch for bonding pads, first upper row	138.92
Pitch for bonding pads, second upper row	138.83
Width of the n zone between the edge of first guard ring p+ zone and n+ zone	300
Width of n+ zone	450

(*) aperture in the passivation layer

W4 HPK

Figure 30: Schematics of the mask design for the W4 detector

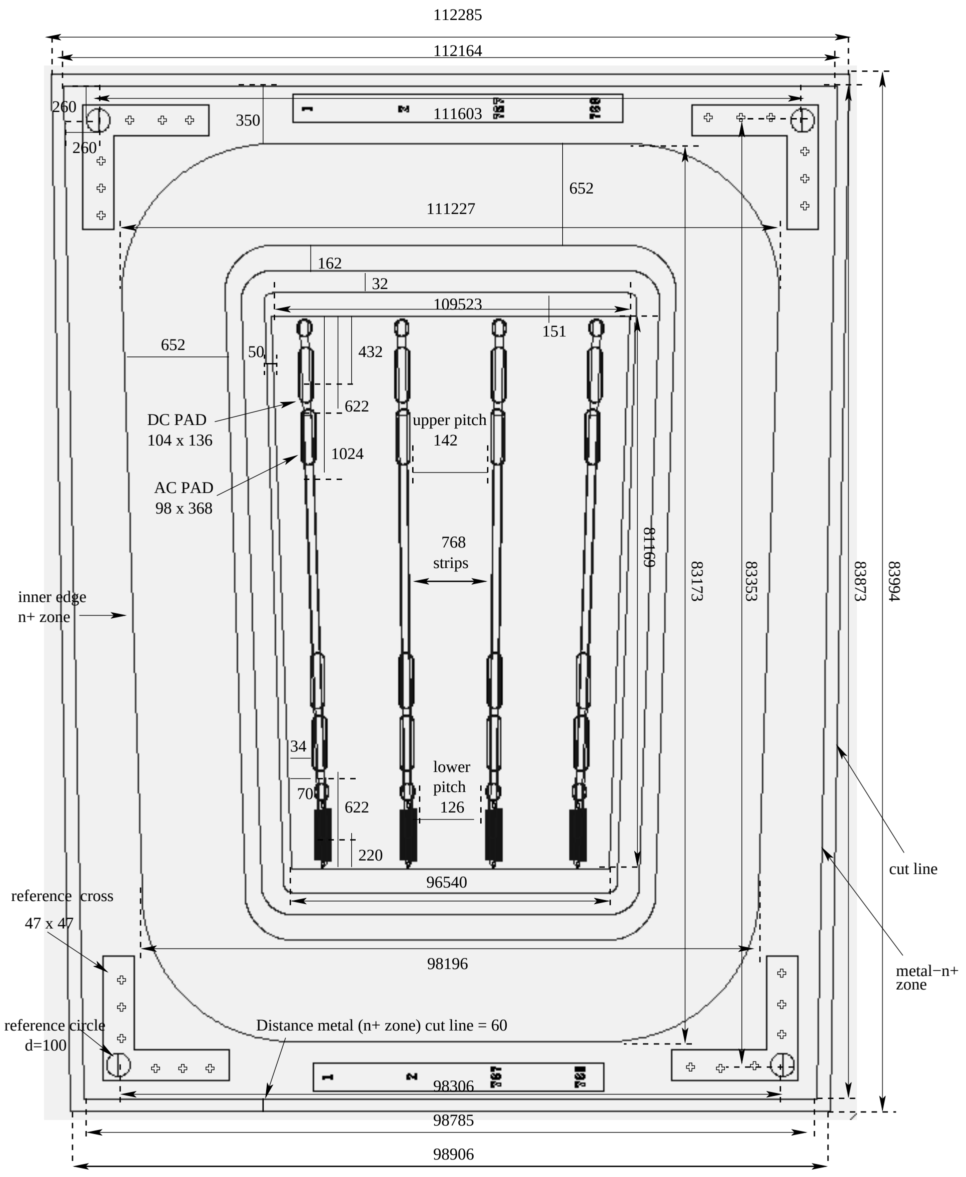

W5A

Dimensions on the sketch are referred to the metal layer
(except for the external cut line).

Parameter	Value (μm)
Overall width (after cutting)	98906-112285
Overall lenght (after cutting)	83994
Active area width	96540-109523
Active area lenght	81169
Strip lenght	80606
Width of strip p$^+$ zone	31-36
Pitch	126-142
Number of strips	768
Width of metal strip	41-48
Distance between end of strip p$^+$ zone and horizontal part of bias ring (lower side)	29
Distance between end of strip p$^+$ zone and horizontal part of bias ring (upper side)	433
Bias pad height (*)	102
Bias pad width (*)	94
Bonding pad height (*)	358
Bonding pad width (*)	88
Pitch for bias pads (lower side)	125.62
Pitch for bonding pads, first lower row	125.66
Pitch for bonding pads, second lower row	125.8
Pitch for bias pads (upper side)	142.37
Pitch for bonding pads, first upper row	142.35
Pitch for bonding pads, second upper row	142.3
Distance between the edge of guard ring p$^+$ zone and n$^+$ zone	700
Width of the n$^+$ zone	410

(*) Dimensions are referred to the opening in the passivation layer

Figure 31: Schematics of the mask design for the W5A detector

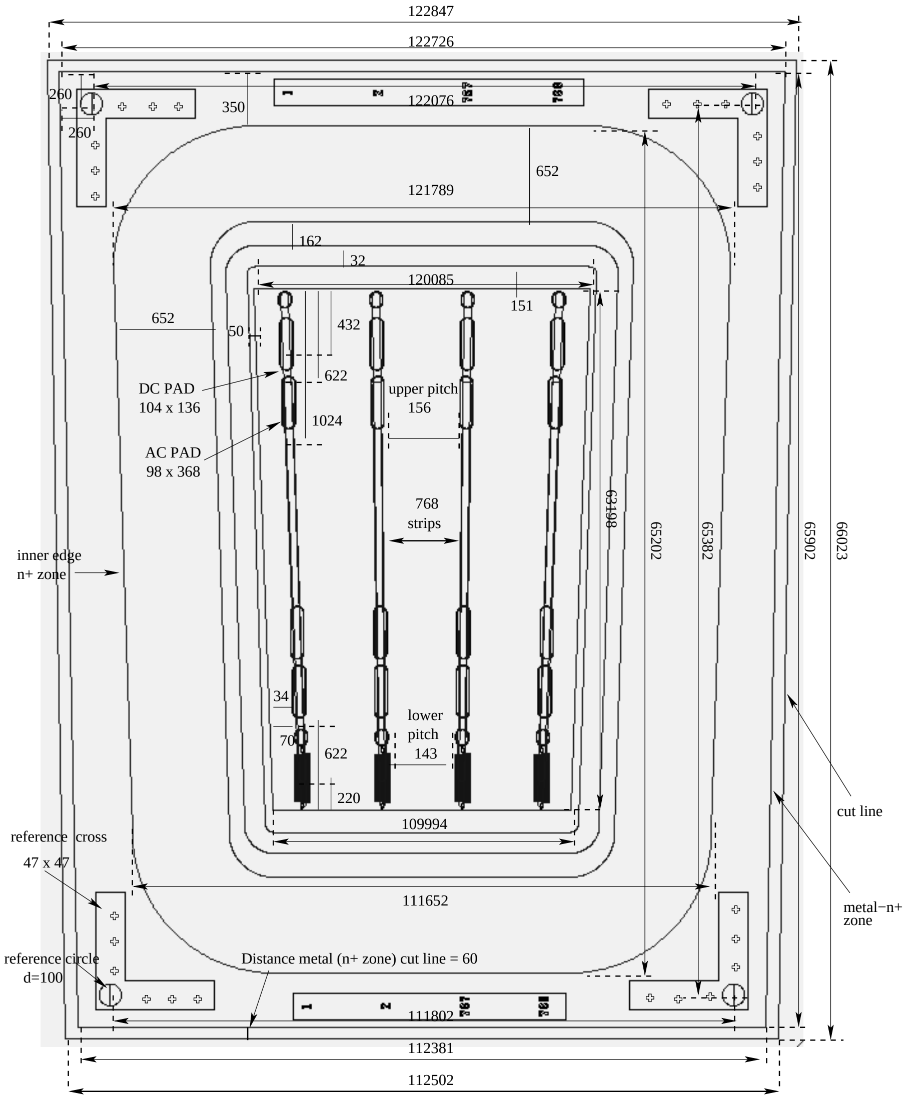

Figure 32: Schematics of the mask design for the W5B detector

W5B

Dimensions on the sketch are referred to the metal layer
(except for the external cut line).

Parameter	**Value (μm)**
Overall width (after cutting)	112502-122847
Overall lenght (after cutting)	66023
Active area width	109994-120085
Active area lenght	63198
Strip lenght	62736
Width of strip p^+ zone	36-39
Pitch	143-156
Number of strips	768
Width of metal strip	46-51
Distance between end of strip p^+ zone and horizontal part of bias ring (lower side)	29
Distance between end of strip p^+ zone and horizontal part of bias ring (upper side)	433
Bias pad height (*)	102
Bias pad width (*)	94
Bonding pad height (*)	358
Bonding pad width (*)	88
Pitch for bias pads (lower side)	143.1
Pitch for bonding pads, first lower row	143.15
Pitch for bonding pads, second lower row	143.3
Pitch for bias pads (upper side)	156.13
Pitch for bonding pads, first upper row	156.13
Pitch for bonding pads, second upper row	156.1
Distance between the edge of guard ring p^+ zone and n^+ zone	700
Width of the n^+ zone	410

(*) Dimensions are referred to the opening in the passivation layer

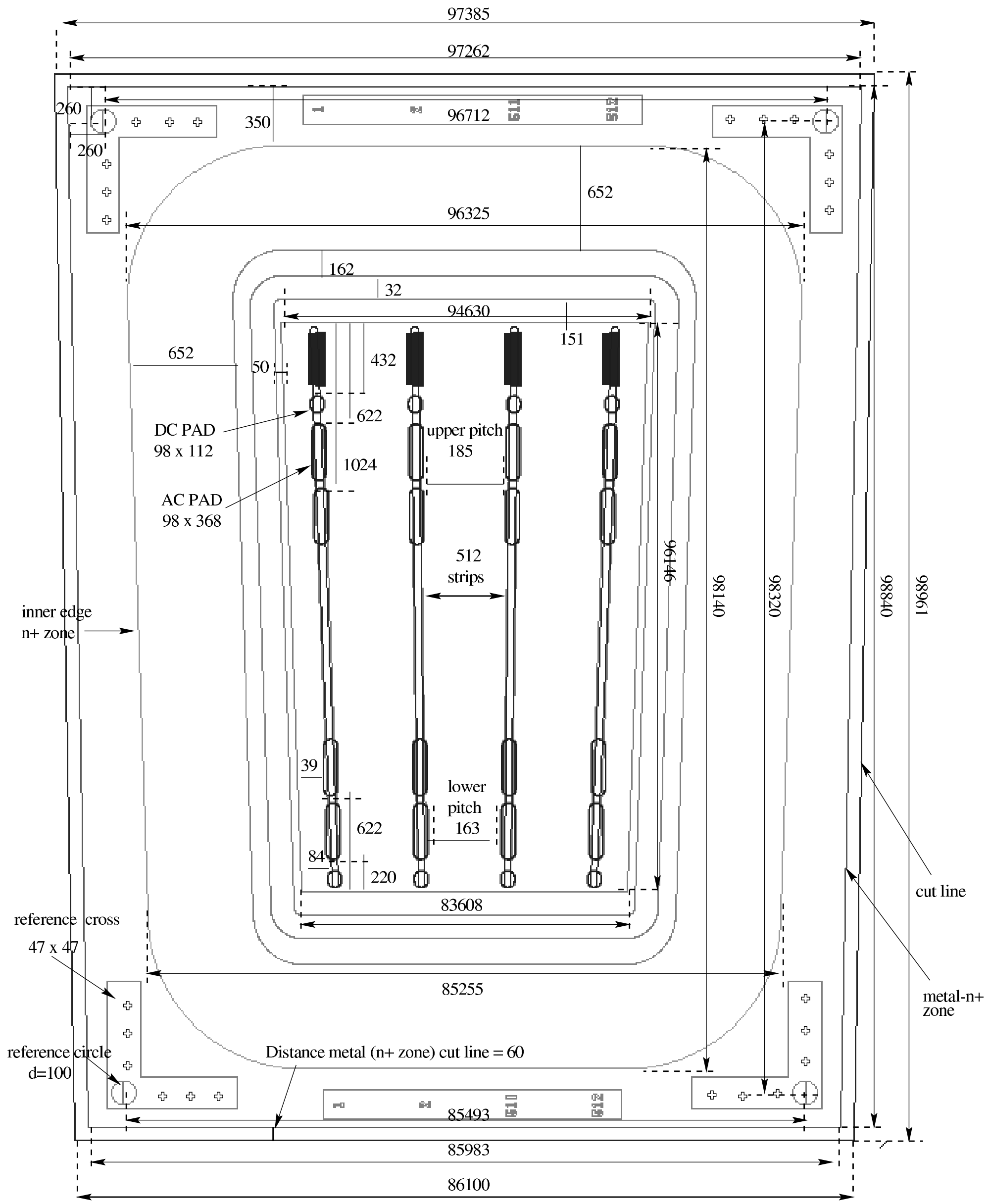

Figure 33: Schematics of the mask design for the W6A detector

W6A

Dimensions on the sketch are referred to the metal layer
(except for the external cut line).

Parameter	**Value (μm)**
Overall width (after cutting)	86100-97385
Overall lenght (after cutting)	98961
Active area width	83600-94620
Active area lenght	96136
Strip lenght	95573
Width of strip p^+ zone	41-46
Pitch	163-185
Number of strips	512
Width of metal strip	53-60
Distance between end of strip p^+ zone and horizontal part of bias ring (lower side)	29
Distance between end of strip p^+ zone and horizontal part of bias ring (upper side)	433
Bias pad height (*)	102
Bias pad width (*)	88
Bonding pad height (*)	358
Bonding pad width (*)	88
Pitch for bias pads (lower side)	163.2
Pitch for bonding pads, first lower row	163.2
Pitch for bonding pads, second lower row	163.4
Pitch for bias pads (upper side)	184.6
Pitch for bonding pads, first upper row	184.6
Pitch for bonding pads, second upper row	184.5
Distance between the edge of guard ring p^+ zone and n^+ zone	700
Width of the n^+ zone	410

(*) Dimensions are referred to the opening in the passivation layer

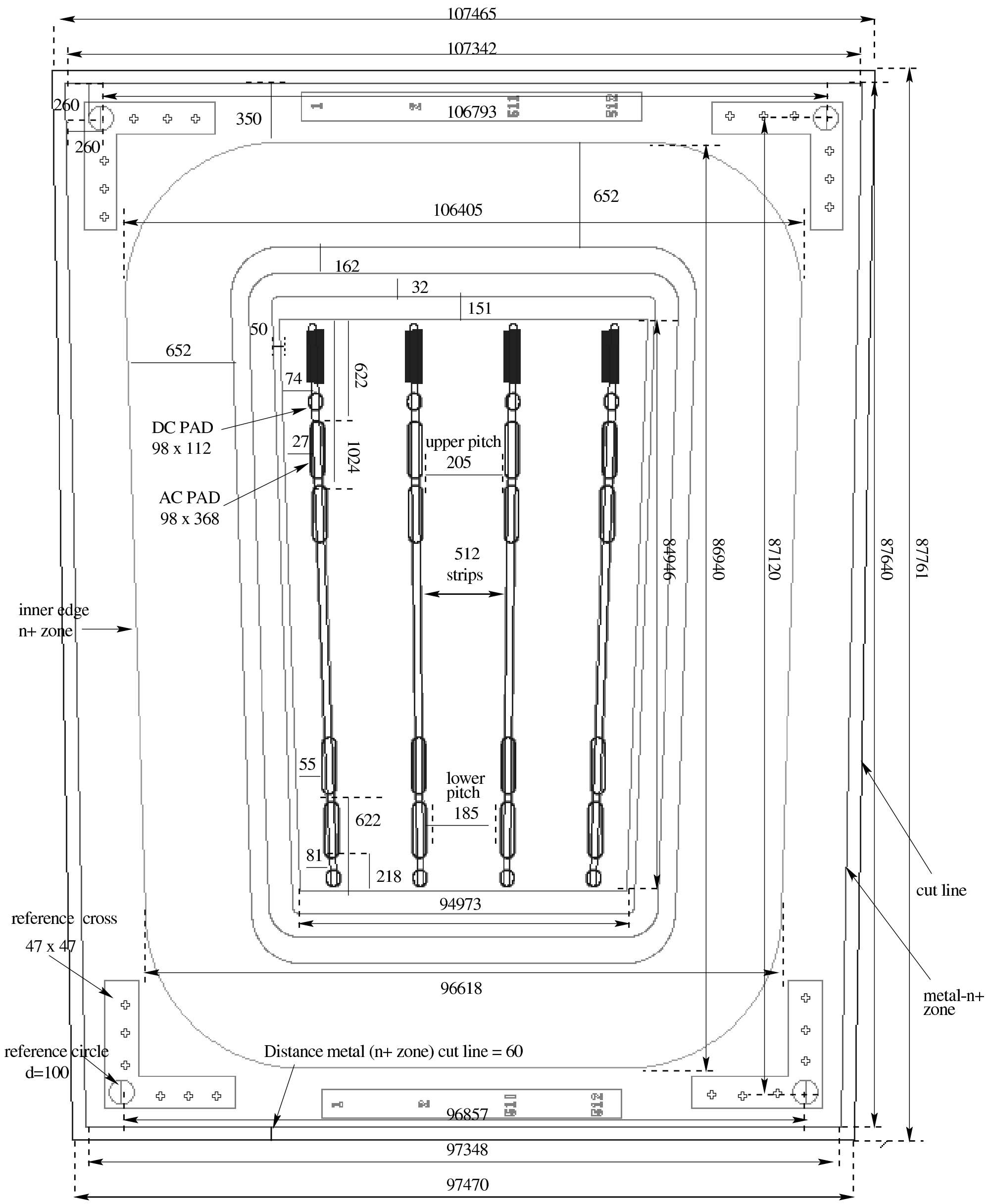

W6B

Dimensions on the sketch are referred to the metal layer
(except for the external cut line).

Parameter	Value (μm)
Overall widht	97470-107465
Overall lenght	87761
Active area width	94963-104701
Active area lenght	84936
Strip lenght	84475
Width of strip p^+ zone	46-51
Pitch	185-205
Number of strips	512
Width of metal strip	60-67
Distance between end of strip p^+ zone and horizontal part of bias ring (lower side)	29
Distance between end of strip p^+ zone and horizontal part of bias ring (upper side)	433
Bias pad height (∗)	102
Bias pad width (∗)	88
Bonding pad height (∗)	358
Bonding pad width (∗)	88
Pitch for bias pads (lower side)	185.5
Pitch for bonding pads, first lower row	185.5
Pitch for bonding pads, second lower row	185.6
Pitch for bias pads (upper side)	204.4
Pitch for bonding pads, first upper row	204.4
Pitch for bonding pads, second upper row	204.2
Distance between the edge of guard ring p^+ zone and n^+ zone	700
Width of the n^+ zone	410

(*) Dimensions are referred to the opening in the passivation layer

Figure 34: Schematics of the mask design for the W6B detector

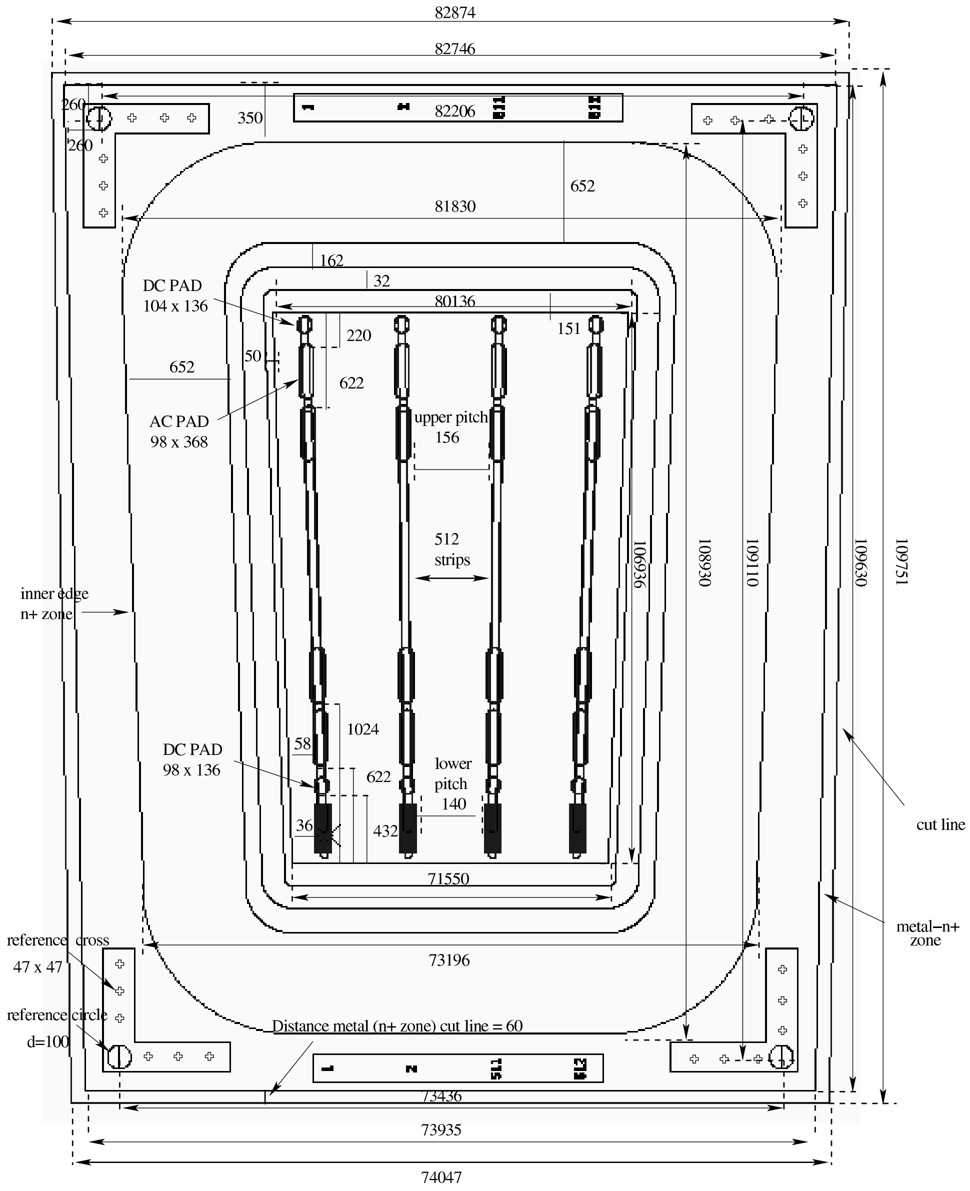

W7A

Dimensions on the sketch are referred to the metal layer
(except for the external cut line).

Parameter	Value (μm)
Overall width (after cutting)	74047-82874
Overall lenght (after cutting)	109751
Active area width	71540-80126
Active area lenght	106926
Strip lenght	106464
Width of strip p^+ zone	35-39
Pitch	140-156
Number of strips	512
Width of metal strip	45-51
Distance between end of strip p^+ zone and horizontal part of bias ring (upper side)	29
Distance between end of strip p^+ zone and horizontal part of bias ring (lower side)	433
Bias pad height (*)	102
Bias pad width (*)	94
Bonding pad height (*)	358
Bonding pad width (*)	88
Pitch for bias pads (lower side)	139.67
Pitch for bonding pads, first lower row	139.67
Pitch for bonding pads, second lower row	139.7
Pitch for bias pads (upper side)	156.35
Pitch for bonding pads, first upper row	156.35
Pitch for bonding pads, second upper row	156.34
Distance between the edge of guard ring p^+ zone and n^+ zone	700
Width of the n^+ zone	410

(*) Dimensions are referred to the opening in the passivation layer

Figure 35: Schematics of the mask design for the W7A detector

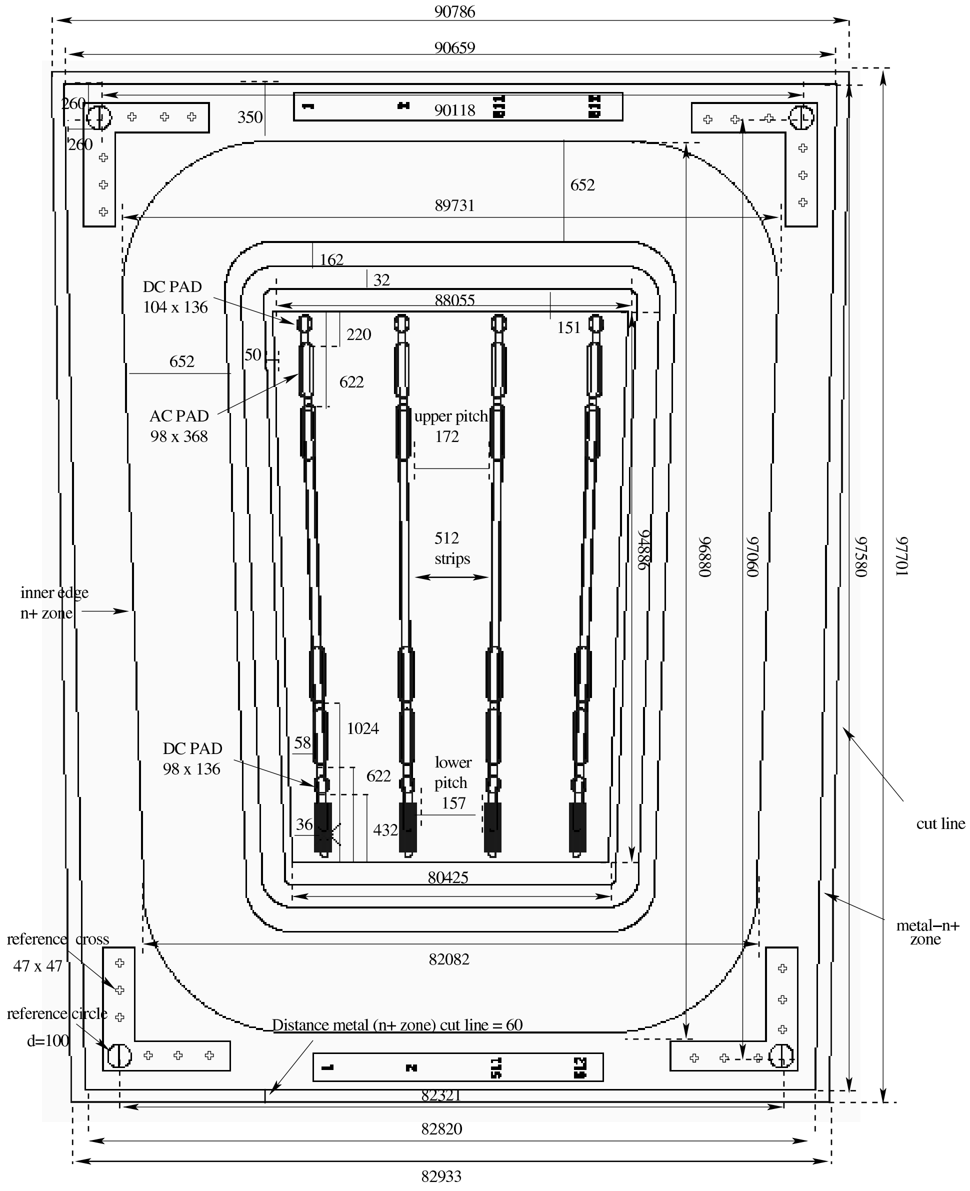

W7B

Dimensions on the sketch are referred to the metal layer (except for the external cut line).

Parameter	Value (μm)
Overall width (after cutting)	82933-90786
Overall lenght (after cutting)	97701
Active area width	80415-88045
Active area lenght	94876
Strip lenght	94414
Width of strip p^+ zone	39-43
Pitch	156-172
Number of strips	512
Width of metal strip	51-55
Distance between end of strip p^+ zone and horizontal part of bias ring (upper side)	29
Distance between end of strip p^+ zone and horizontal part of bias ring (lower side)	433
Bias pad height (*)	102
Bias pad width (*)	88
Bonding pad height (*)	358
Bonding pad width (*)	88
Pitch for bias pads (lower side)	157
Pitch for bonding pads, first lower row	157
Pitch for bonding pads, second lower row	157.01
Pitch for bias pads (upper side)	171.76
Pitch for bonding pads, first upper row	171.76
Pitch for bonding pads, second upper row	171.74
Distance between the edge of guard ring p^+ zone and n^+ zone	700
Width of the n^+ zone	410

(*) Dimensions are referred to the opening in the passivation layer

Figure 36: Schematics of the mask design for the W7B detector